LIGHT-EMITTING DIODES

M. GEORGE CRAFORD AND FRANK M. STERANKA, *Optoelectronics Division, Hewlett-Packard Company, San Jose, California, U.S.A.*

INTRODUCTION

A light-emitting diode (LED) is a semiconductor device that emits visible or infrared radiation when electric current is passed through it. The basic device consists of a single *p-n* junction. The energy of the emitted photons, which determines the color, is usually approximately equal to the energy gap of the semiconductor material in the active region of the LED. Materials that are generally used for LEDs are compounds of elements from columns III and V of the periodic chart such as GaAs, GaP, AlGaAs, InGaP, GaAsP, GaAsInP, and more recently AlInGaP . The specific material is chosen on the basis of color, performance, and cost. A cross section of a LED lamp is shown in Fig. 1. The semiconductor chip is typically $250 \times 250\ \mu m^2$ and is mounted on one of the electrical leads. A bond wire electrically connects the top of the chip to the other lead. The epoxy dome serves as a lens to focus the light and as a structural member to hold the device together. Operating currents are usually in the range of 1–50 mA, and forward voltages are about 2 V.

The external quantum efficiency (photons out per electron passed through the device), which is roughly equal to the power efficiency of visible LEDs, ranges from less than 0.1% to more than 10%. The luminous performance of visible LEDs is obtained by multiplying the power efficiency by the eye sensitivity curve as defined by the Commission Internationale de L'Eclairage, or CIE. LEDs typically have performance in the range of 1–10 l/W, but LEDs with performance as high as 20 l/W have been observed. This compares favorably with incandescent bulbs that are typically in the range of 15 l/W. LEDs usually operate at power levels of less than 0.1 W, and so they are not suitable for room illumination. However, they are widely used for large-area displays and for exterior lighting on vehicles.

The evolution of visible LEDs is shown in Fig. 2. Red GaAsP LEDs were first introduced commercially by General Electric in 1962 in very low volumes following the work of Holonyak and Bevacqua (1962). High-volume production of GaAsP emitters began in 1968 (Herzog *et al.*, 1969) and was soon followed by the introduction of GaP:(Zn,O) LEDs (Saul *et al.*, 1969). Both of these types of emitters had efficiencies of approximately 0.1 l/W and were only available in the color red. In the late 1960s and early 1970s, it was discovered that nitrogen provided an efficient recombination center in both GaP (Logan *et al.*, 1968) and GaAsP (Groves *et al.*, 1971). This led to the commercial introduction in the mid-1970s of red, orange, yellow, and green GaAsP:N and GaP:N LEDs with performance in the range of 1 l/W. Early work (Rupprecht *et al.*, 1967, Alfërov *et al.*, 1973) had indicated that AlGaAs and heterostructure AlGaAs LEDs offered potential performance advantages over GaAsP

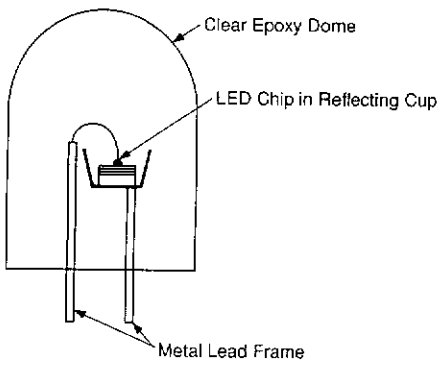

FIG. 1. Cross sectional view of a typical LED lamp. The LED chip, typically $250 \times 250 \times 250\ \mu m^3$, is mounted in a reflective cup formed in a lead frame. Clear epoxy acts as a lens, an index-of-refraction matching medium to help extract light from the chip, and a structural member to hold the package together.

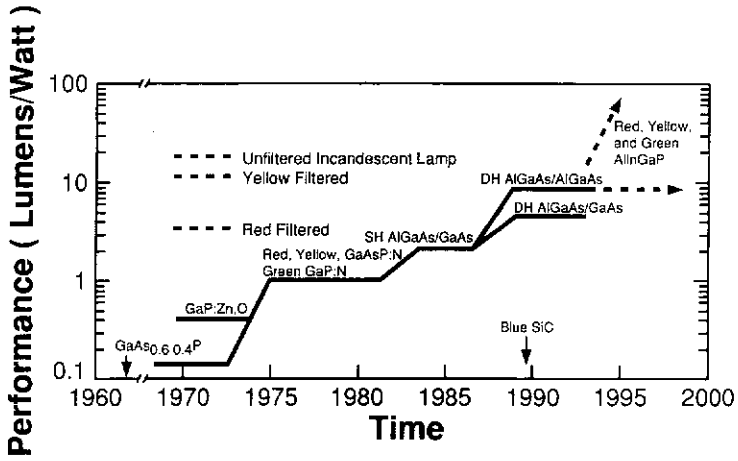

FIG. 2. Schematic illustration of the evolution of visible LEDs. Early LEDs only emitted red. The addition of nitrogen doping in GaAsP (GaAsP:N) improved red performance, and made orange and yellow possible. In GaP, nitrogen doping (GaP:N) made green available, and during the 1980s, GaP gradually improved to ~2.5 l/W (not shown). Double-heterostructure (DH) red-emitting AlGaAs devices now offer better performance than red-filtered incandescents and are used in some automobile taillights. AlInGaP has the potential to be brighter than AlGaAs in yellow and possibly red and green.

and GaP homojunctions. However, more than a decade of development was required to create high-volume liquid-phase–epitaxy (LPE) reactors capable of growing high-quality multilayer device structures (Nishizawa and Suto, 1977). It was not until the early 1980s that such LEDs became commercially available. The performance of these LEDs ranged from 2 to 10 l/W (depending upon the structure employed), and for the first time, LEDs broke the efficiency barrier of filtered incandescent bulbs, enabling them to replace light bulbs in many outdoor lighting applications.

Finally, in the early 1990s orange and yellow AlInGaP devices with efficiencies greater than 10 l/W were developed (Kuo *et al.*, 1990). The growth of such LEDs by conventional techniques such as LPE or halide-transport vapor-phase epitaxy proved intractable. The emergence of metal-organic vapor-phase epitaxy (MOVPE) as a crystal-growth technique beginning in the late 1960s (Manasevit and Simpson, 1969) and yielding high-performance AlGaAs devices in the late 1970s (Dupuis and Dapkus, 1977) later made possible the controlled growth of heterostructure AlInGaP LEDs. Their performance is expected to improve significantly over the next decade as more is learned about this crystal-growth process.

Blue SiC LEDs are also available but they are much less efficient than the other types. The development of brighter blue LEDs, possibly using ZnSe or GaN, which have shown promise in the research laboratory, is expected to be a major development area in the 1990s.

The discovery that diffused-junction GaAs diodes were efficient sources of infrared radiation (Keyes and Quist, 1962) led to the commercial introduction of infrared LEDs in the early 1960s as well. These Zn-diffused GaAs diodes had typical external quantum efficiencies of approximately 1% in air. In 1966 it was discovered (Rupprecht *et al.*, 1966) that Si-doped GaAs diodes with grown-in p-n junctions could provide efficiencies greater than 6%. Even higher efficiencies (up to 12%) were obtained by silicon doping a thick AlGaAs layer and then removing the original (absorbing) GaAs substrate (Dawson, 1977). Plastic-encapsulated GaAs:Si and AlGaAs:Si LEDs such as these have output powers in the 12–26-mW range when driven at 100 mA and can be reliably driven at peak currents up to 1.5 A. They have been extensively used in remote control applications for TVs and VCRs. Their switching times, however, are quite long (approximately 1 μs), and so they are unsuitable as sources for high-speed data communi-

cation. The need for fast light sources that could be used in fiber-optic links led to the development of small-area, high-radiance AlGaAs and InGaAsP LEDs in the 1970s and 1980s (see Saul *et al.*, 1985; Pearsall, 1982). They are used in medium-distance (< 10 km) and low–data-rate (10 to 200 Mbit/s) applications while semiconductor lasers are used for longer-distance or higher–data-rate communications.

1. BASIC DEVICE PHYSICS

1.1 *p-n* Junction

The basic structure of an LED is among the simplest of semiconductor devices since it consists of a single *p-n* junction, where *p*-type (excess positive charge carriers called holes) and *n*-type (excess electrons or negative charge carriers) semiconductor materials are in single-crystal contact with each other as indicated in Fig. 3. When the junction is biased in the forward direction, electrons are injected into the *p*-type region, and/or holes are injected into the *n*-type region. These injected minority carriers can then recombine with majority carriers, giving up energy.

When biased in the forward direction, LED junctions begin to conduct significantly at voltages approximately equal to the semiconductor energy gap of the material involved. This can range from 0.8 to 1.5 V for infrared emitters and from 1.5 to more than 3.0 V for visible emitters (see Secs. 3.2.1 and 4.2.1). The reverse breakdown voltage is generally limited by the carrier concentration in the *n*-type region and can range from 5–10 V for heavily-doped devices to more than 50 V for many types of visible emitters.

The slope of the current-voltage characteristic after turn-on in the forward direction is known as the dynamic resistance. The dynamic resistance is determined by the area of the junction, the Ohmic-contact technology, and the conductivity of the semiconductor materials involved. The dynamic resistance can range from about 1 Ω for an IR device designed for high-current operation to 10 Ω or

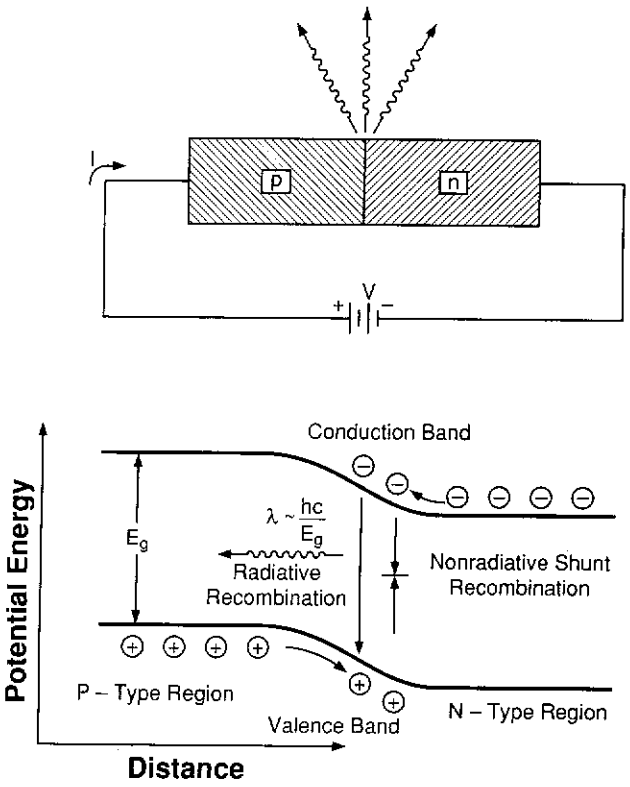

FIG. 3. Schematic of an LED and forward-biased LED junction. Radiative processes, which result in photon emission, and nonradiative processes, which generate heat, are illustrated. In indirect–band-gap material they are forbidden. Reprinted from Tannas (1985), courtesy of Van Nostrand Reinhold Company, Inc. Copyright © 1985.

more for a visible LED that is optimized for high light-output efficiency and designed to operate at 30 mA or less.

1.2 Radiative and Nonradiative Recombination and Internal Quantum Efficiency

When injected minority carriers recombine with majority carriers, the energy can be converted into either light or heat, depending upon whether the recombination is "radiative" or "nonradiative" as shown in Fig. 3. Typical radiative and nonradiative recombination processes are listed in Table 1. The internal quantum efficiency of the LED, the number of photons generated divided by the number of minority carriers injected, is determined by the relative radiative and nonradiative recombination rates. This is shown below for the case of electron injection into a p-type active region, which is generally the case for LEDs. The total recombination rate for electrons can be expressed as the number of electrons, n, divided by a characteristic lifetime τ:

Table 1. Examples of recombination routes.

Radiative	Nonradiative
Band to band	Phonon emission
Band to acceptor	At dislocations
Donor to acceptor	At impurities
Through isoelectronic centers	At lattice vacancies
	At interstitials

$$\text{Total recombination rate} = n/\tau = \text{radiative rate} + \text{nonradiative rate} = n/\tau_r + n/\tau_{nr}$$

$$= n(1/\tau_r + 1/\tau_{nr}),$$

where τ_r and τ_{nr} are the radiative and nonradiative decay times, respectively.

$$\text{Internal quantum efficiency} = \eta_{int} = \frac{\text{radiative rate}}{\text{total recombination rate}},$$

$$\eta_{int} = \frac{n/\tau_r}{n/\tau} = \frac{1/\tau_r}{1/\tau_r + 1/\tau_{nr}}.$$

Therefore

$$\eta_{int} = \frac{1}{1+\tau_r/\tau_{nr}}.$$

In order to have high-performance devices, we want τ_{nr} to be large compared to τ_r The nonradiative lifetime is determined by the quality of the material, and if the nonradiative paths shown in Table 1 are minimized, τ_{nr} can be as long as a microsecond or even longer; but even in good material, τ_{nr} is more typically in the tens of nanoseconds range.

We would like to have τ_r as small as possible. At low minority-carrier injection levels, the radiative recombination rate can also be expressed as $n/\tau_r = Bnp$ or $\tau_r = 1/Bp$ where B is the recombination rate constant for a given type of semiconductor material, and n and p are the electron and hole concentrations. In order to reduce τ_r we want to have the hole concentration p as large as possible without degrading the quality of the material and hence decreasing τ_{nr}. When materials are doped above a maximum hole concentration, which is different for different materials, and can range from about 10^{17} to 10^{19} cm^{-3}, the material quality is degraded, and τ_{nr} decreases sharply.

The radiative constant is determined by the material system involved. For GaAs, B is about 2×10^{-10} cm^3/s^{-1} (Casey and Panish, 1978). Thus if $p=10^{18}$ cm^{-3}, $\tau_r = 1/Bp = 5\times10^{-9}$ s which is a typical radiative decay time for a GaAs device. The nonradiative decay time for good-quality GaAs material is generally 10^{-7} s or longer so that the internal quantum efficiency approaches 100%. In most semiconductors, the internal quantum efficiency is much lower than 100% because of material quality problems or the fact that the recombination constant is smaller. The latter is the case for indirect materials where B can be orders of magnitude smaller as described in Sec. 1.3. The external quantum efficiency, which is the internal quantum efficiency mul-

tiplied by a light extraction factor, is lower, sometimes by more than an order of magnitude, than the internal efficiency because of the difficulty in extracting light from the interior of the LED chip. This is discussed in Sec. 1.8.

1.3 Direct and Indirect Energy Gap

The energy gap of a semiconductor is the minimum separation between the valence band, which is the continuum of allowed energy versus momentum states for the holes or *p*-type charge carriers, and the conduction band, which is the same characteristic for the electrons. This energy gap is the primary factor that determines the color of an LED, as described in Sec. 1.6. However, the separation between the conduction band and the valence band changes as a function of the momentum of the electrons and holes, and the relative momenta of the electrons and holes at the point where the energy-gap separation is a minimum is a key factor in determining the suitability of the material for the fabrication of efficient LEDs.

In a direct semiconductor, the minimum energy gap occurs at the point where both the electrons and holes have zero momentum. The electrons and holes are concentrated around this region as shown in Fig. 4. Radiative recombination occurs readily in this situation since the electrons and holes can recombine emitting a photon that has an energy equal to that given up in the recombination process—thus conserving energy. Momentum is also conserved since the photon has negligible momentum and both the electron and hole had nearly zero momentum in the beginning.

In an indirect semiconductor, on the other hand, the electrons and holes have different momenta at the point where the band separation is a minimum. The holes are still concentrated in a region with nearly zero momentum, but the electrons are concentrated in the conduction-band minimum with non-zero momentum as shown in Fig. 4. In this situation, radiative transitions can no longer readily occur. Although energy conservation can be achieved with the emission of a photon, momentum conservation cannot, since photons have nearly zero momentum and cannot make up for the momentum difference between the electron and hole.

Radiation can only occur in indirect semiconductors with the involvement of an additional interaction that allows momentum to be conserved. This interaction can occur with lattice vibrations (phonons) resulting in heat being transferred to or absorbed from the crystal lattice. This process yields an emitted photon with an energy that is different from the energy gap by an amount equal to the energy of the phonon that is simultaneously generated or absorbed. Processes of this type are relatively unlikely compared to direct recombination, and so τ_r is longer, the ratio τ_r/τ_{nr} is larger, and high quantum efficiencies are difficult to achieve in pure indirect semiconductors.

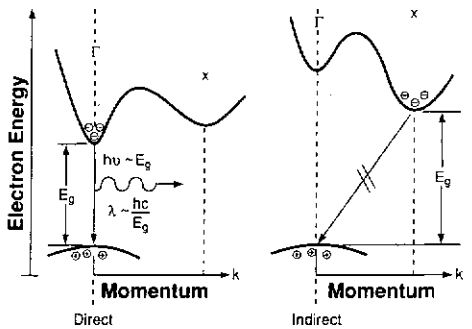

FIG. 4. Schematic diagram of conduction and valence bands in direct and indirect semiconductors. Electron energy is plotted as a function of momentum (k). In direct-band-gap material band-to-band radiative transitions are allowed. In indirect-band-gap material they are forbidden. Reprinted from Tannas (1985), courtesy of Van Nostrand Reinhold Company, Inc. Copyright © 1985.

1.4 Isoelectronic Impurities

In spite of the problem presented by the band structure, indirect semiconductors are widely used for LEDs. Acceptable quantum efficiencies are achieved by intentionally adding isoelectronic impurities, which act as radiative recombination centers, to the crystal. An "isoelectronic" impurity comes from the same column of the periodic chart as the host crystal, and hence it has an electronic charge no different from that of the element it replaces. The isoelectronic impurity introduces a highly localized region of strain in the crystal that traps an electron. Since the trap is highly localized, the uncertainty in position is small and so, according to the Heisenberg

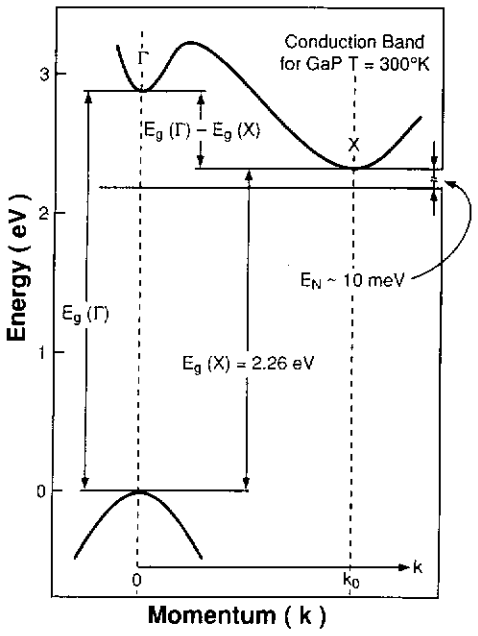

FIG. 5. Energy-band structure for an indirect semiconductor with an isoelectronic impurity (GaP with nitrogen doping is shown). The shaded region shows the probability distribution for an electron associated with the nitrogen impurity, and it can be seen that there is a significant probability that the electron will be near zero momentum so that it can recombine radiatively. Reprinted from Tannas (1985), courtesy of Van Nostrand Reinhold Company, Inc. Copyright © 1985.

uncertainty principle, the uncertainty in momentum is large. Thus, electrons trapped at isoelectronic impurities are widely distributed in momentum, and there is a significant probability that the electrons can have zero momentum and can combine radiatively. This situation is illustrated in Fig. 5 for GaP with nitrogen doping. Even with the addition of isoelectronic impurities, however, the recombination lifetime is longer than that for direct semiconductors, and the internal quantum efficiencies are typically much less than 100%.

1.5 Direct–Indirect Transition

Ternary (three-element) and quaternary (four element) alloys are used for many types of LEDs. Examples are $GaAs_{1-x}P_x$, $Al_xGa_{1-x}As$, and $(Al_xGa_{1-x})_{0.5}In_{0.5}P$. The energy gap changes with alloy composition, and, in many cases, a transition from a direct-band-gap to an indirect-band-gap semiconductor occurs at some composition (x_c). This is illustrated in Fig. 6. The quantum efficiency of the LEDs changes, typically by orders of magnitude, as this transition is crossed. The quantum efficiency as a function of alloy composition can be calculated if we assume that only electrons in the direct conduction-band minimum can recombine radiatively and that the nonradiative lifetime is the same for both direct and indirect electrons.

The total number of electrons is equal to the number of electrons in the direct minimum plus the number of electrons in the indirect minima:

$$n = n_D + n_I.$$

According to Boltzmann statistics, the ratio of the number of electrons in the indirect minima to the number in the direct minimum can be written

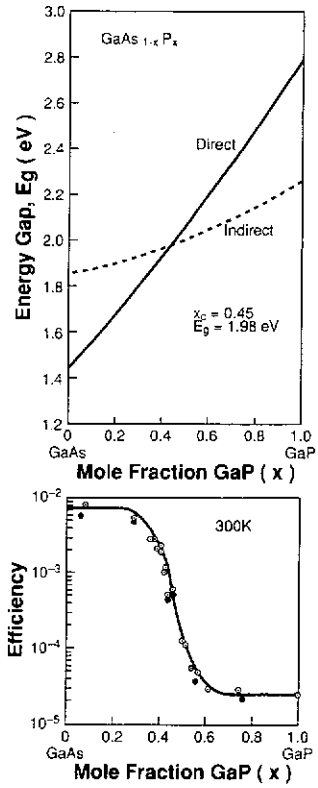

FIG. 6. Direct and indirect energy gaps plotted as functions of alloy composition. The quantum efficiency is high in the direct region to the left of the direct-indirect transition, and is orders of magnitude lower to the right. The data points are from Herzog *et al.*, 1969.

$$F = n_I/n_D = Ne^{-\Delta E(x)/kT},$$

where F is the fraction of carriers in the indirect minima, N is the relative density of states in the indirect minima (typically N is >10), and $\Delta E(x)$ is the separation between the direct and indirect minima.

Now, the radiative recombination rate $= n_D/\tau_r$, the nonradiative recombination rate $= n_I/\tau_{nr} + n_D/\tau_{nr} = n/\tau_{nr}$, and therefore

internal quantum efficiency

$$= \eta_{int} = \frac{n_D/\tau_r}{n_D/\tau_r + n/\tau_{nr}}$$

$$= \frac{1}{1 + (\tau_r/\tau_{nr})(1 + Ne^{-\Delta E/kT})}.$$

The quantum efficiency now depends on the lifetime ratio as well as the fraction of carriers in the indirect minima and drops exponentially as the separation between the minima becomes small.

1.6 Emission Wavelength versus Energy Gap and Doping

The wavelength of an LED is inversely proportional to the energy of the emitted photon, E, according to the relationship $\lambda = hc/E$, where λ is the wavelength of light, h is Planck's constant, and c is the velocity of light. The energy of the photon is equal to the energy gap if free electrons and holes are recombining, or to the energy gap minus the energy of the trap, impurity level, or phonon if these processes are involved. This can be represented as $\lambda = hc/(E - E_x)$ where E_x is the energy of the trap, etc. Typical n-type dopants have level depths of a few thousandths of an electron volt and p-type dopants have depths of a few tens of thousandths of an electron volt, both of which are small compared to the band gaps of LEDs. Therefore for most types of LEDs, the peak emission wavelength $\lambda \approx hc/E_g$. This is not necessarily the case for materials with isoelectronic traps, which can have trap depths of more than 0.1 eV.

1.7 Device Structures

1.7.1 Homojunctions. The simplest and generally least-expensive LEDs are homojunctions in which the entire epitaxial structure, and sometimes the substrate, consists of the same compound or alloy composition. Examples of common homojunction LEDs are given in Table 2, and a GaP homojunction device is shown in Fig. 7(a). The p-n junction can be formed by p-type diffusion into an n-type epitaxial film, or can be grown by changing the dopant type during the epitaxial growth process.

The optimum junction depth is a compromise between two conflicting requirements.

Table 2. Types of LEDs grouped by structure type.

Structure	Epitaxial layer /Substrate	Desirable device characteristics: Low defect density	Good injection efficiency	Good carrier confinement	Low internal absorption	Manufacturability
Homojunction	GaAsP/GaAs	No	No	No	No	Excellent
	GaAsP:N/GaP	No	No	No	Yes	Excellent
	GaP:(Zn,O)/GaP	Yes	No	No	Yes	Excellent
	GaP:N/GaP	Yes	No	No	Yes	Excellent
	GaAs:Si/GaAs	Yes	No	No	Yes	Excellent
Single heterostructure	AlGaAs/GaAs	Yes	Yes	No	No	Good
Double heterostructure	AlGaAs/GaAs	Yes	Yes	Yes	No	Good
	AlGaAs/AlGaAs	Yes	Yes	Yes	Yes	Fair but improving
	AlInGaP/GaAs	Yes	Yes	Yes	No	New (TBD)[a]

[a]TBD stands for "to be determined"

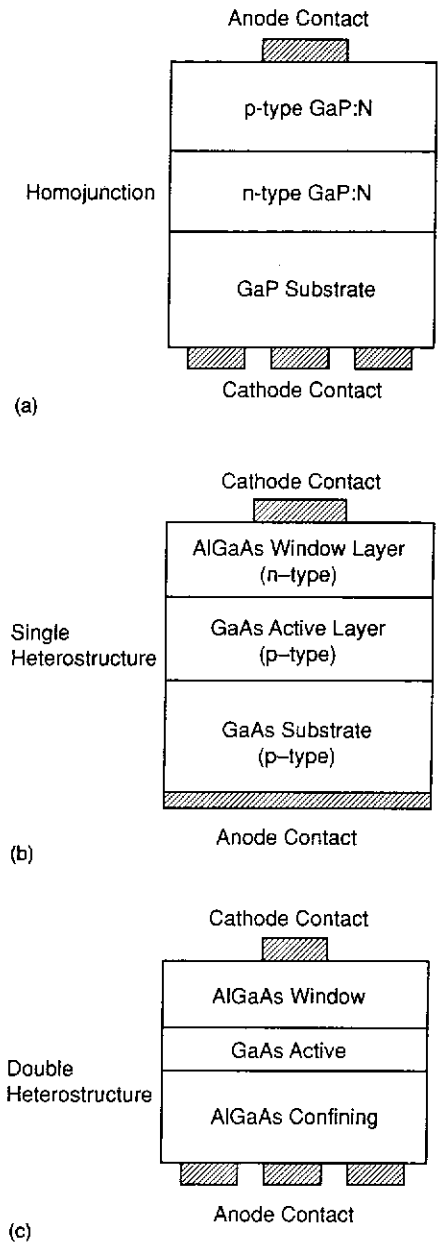

FIG. 7. Cross sections of various types of LED structures. (a) The simplest type is a homojunction in which both the *p*-type and *n*-type regions are similar material as in a GaP:N LED. (b) A single heterostructure has different material compositions on the *p*-type and *n*-type sides as in an AlGaAs/GaAs LED. (c) A double heterostructure has an additional layer on the other side of the active layer to confine the injected electrons and/or facilitate light extraction.

The junction must be deep enough so that only a small fraction of the injected carriers reaches the surface (where they generally recombine nonradiatively), and so that the sheet conductivity of the *p*-type region is high enough to avoid current crowding around the contact. On the other hand the junction should be as shallow as possible to minimize absorption. This latter requirement is particularly important for direct–band-gap devices because the absorption coefficient for near–band-gap radiation is $\sim 10^4$ cm^{-1}. Consequently, junctions in direct–band-gap homojunctions, which utilize a near-band-edge recombination processes, are generally less than 3 μm deep.

In the case of indirect semiconductors, the absorption coefficient near the band edge is only $\sim 10^3$ cm^{-1}, and the junction can be deeper. In addition, most indirect–band-gap LEDs utilize isoelectronic impurities where the transition energy is below the band edge and the absorption is substantially reduced. Consequently, in indirect–band-gap LEDs, the junction depth is often more than 10 μm, particularly for devices with grown-in junctions. The doping levels on the *p* and *n* sides of the junction are optimized both to maximize the injection of minority carriers into the preferred active region of the devices and to have the radiative lifetime in the active region be as short as possible to minimize nonradiative recombination. These are also conflicting requirements. The *p*-type region is generally the preferred active region, and it would be desirable to dope it as heavily as possible, without introducing crystal damage, in order to minimize the radiative lifetime relative to the nonradiative lifetime. It would also be desirable to dope the *n*-type region heavily to achieve effective injection. In practice it is generally found that heavy *n*-type doping results in shortened nonradiative lifetimes, and so the desired doping level cannot be achieved and device efficiency is compromised. Many of the limitations of homojunctions can be overcome with the formation of heterostructures.

1.7.2 Single Heterostructures. A single-heterostructure device has two different materials or alloy compositions on opposite sides of the junction. Devices of this type are generally not much more difficult to produce than homojunction LEDs, and they have several advantages. Consider, for example, a device

with an *n*-type AlGaAs "window layer" grown on a *p*-type GaAs active layer (or AlGaAs layer of lower aluminum concentration) as shown in Fig. 7(b). The AlGaAs layer has a higher band gap and is transparent to the radiation generated in the GaAs active layer. Therefore the AlGaAs layer can be thick enough to give good current spreading and a minimum of surface recombination. Furthermore, efficient injection can be achieved since it is energetically favorable for the electrons to flow from the wider-band-gap region into the lower-energy-gap active region even if the *n*-type region is much more lightly doped than the *p*-type region. One limitation of this structure is that some of the injected electrons can penetrate quite deeply into the *p*-type region before they recombine, and much of the radiation that is generated will be absorbed before it can escape. Also, any radiation that is emitted downward will be absorbed. These limitations can be minimized with the growth of appropriate double heterostructures.

1.7.3 Double Heterostructures. The LED structure with the best efficiency is a double heterostructure in which an active region with a lower energy gap is sandwiched between two layers with higher energy gaps: an upper "window" layer and a lower "confining" layer. This structure has the advantages of a single heterostructure and, in addition, reduces the absorption of the generated radiation. The active region can be quite thin, typically 1–3 μm, since the wider band gap of the "confining" layer keeps the injected electrons from penetrating beyond the heterostructure interface. The confinement of the carriers to a narrow region results in fast and efficient recombination. The issue of fast recombination is important primarily for applications related to electronic switching or communication. Devices for these applications also often have small junction areas to minimize capacitance.

The thin active region minimizes absorption, and if the confining layer is relatively thick, some of the light that is generated can escape from the edges of the confining layer, thereby increasing the external efficiency of the device. Optimally the confining layer is grown thick enough (> 100 μm) so that the substrate can be removed altogether [see Fig. 7(c)], resulting in a "transparent substrate" which gives the optimal efficiency as described in Sec. 1.8.1.

An alternative approach to growing a thick confining layer is to grow a Bragg reflector, using alternate one-quarter-wavelength-thick layers of semiconductor material with different indices of refraction in order to reflect the light back up into the chip instead of going down into the substrate. These reflectors are very effective for nearly on-axis radiation but are not effective for low-angle reflections. Therefore they work very well for surface emitting lasers but are less effective for LEDs than transparent substrates. The only disadvantage of double heterostructures compared to the structures described earlier is that they are more complicated and difficult to grow, thus adding to the cost. The thin active region and Bragg reflector layers, if utilized, may be harder to control in a production environment. Thick confining and/or transparent substrate layers are also somewhat harder to control and add time and cost. However, as production technology evolves, many of these structures will become more widely used.

1.7.4 Quantum Wells and Other Structures. LEDs with complex active regions containing one or more quantum wells have been fabricated. These structures, which are widely used for injection lasers, could give better LEDs since less absorption might be expected and injected-carrier densities in the active regions can be higher, resulting in fast radiative recombination. However, it has generally been found that the benefits gained from the added complexity are less for LEDs than lasers and have been more than offset by the anticipated cost and difficulty encountered in producing devices of this type in high volume. Consequently, devices of this type are not widely used in LED applications at this time but may become more viable in the future.

1.8 LED Performance and Extraction Efficiency

The usefulness of an LED depends upon its external performance. For visible LEDs this performance is generally expressed in terms of the luminous flux emitted divided by the power input, in units of lumens/watt. For infrared LEDs the performance is determined by the external quantum efficiency (the ratio

of number of photons emitted to the number of electrons injected) expressed in percent, or as power efficiency (watts output divided by watts input), also expressed as a percentage. This section discusses the issues related to extracting radiation from the LED chip and the relationships between internal quantum efficiency, power efficiency, and luminous performance.

1.8.1 Light Extraction. The external efficiency of LEDs is much lower than the internal efficiency because of the difficulty of extracting light from the semiconductor chip. The ratio of external quantum efficiency to internal quantum efficiency can be defined as an extraction ratio R_E. The problem of internal absorption for different types of structures was discussed in Sec. 1.7, and extraction efficiencies for different types of LED structures are summarized in Table 3. Internal absorption is a major problem for LEDs because the semiconductor chip has an index of refraction of about 3.5, resulting, according to Snell's Law, in a critical angle $[\theta_c = \sin^{-1}(n_1/n_2)]$ for internal reflection of typically 17° when the chip is in air. In most cases, the LED chip is encapsulated in epoxy, with an index of about 1.5, and this critical angle increases to about 25°. Nevertheless, for the case of an LED on an absorbing substrate with a thin epitaxial layer such that edge emission is negligible, only the light that is emitted upward within a cone of 25° will escape from the chip. The extraction ratio for this upward cone can be calculated to be $(1-\cos\theta_c)/2$. One must also correct for Fresnel reflection losses $(n_1/n_2-1)^2/(n_1/n_2+1)^2$ at each interface (assuming normal incidence). The emission cone gives an extraction ratio of 0.05 and Fresnel losses are about 0.2, counting both interfaces. This results in an extraction ratio of only 0.04, or an external quantum efficiency of 4% even if the internal quantum efficiency is 100%. To make matters worse, the presence of the electrical contact on top of the chip can also block much of the light so that the extraction ratio can be substantially less than 0.04. However, in well-designed LEDs, the epitaxial layer is from several micrometers to several tens of micrometers thick, to get both good current spreading and edge emission, and the extraction ratio can be more than 0.1 even for absorbing-substrate devices.

In the case of transparent-substrate devices, much of the light that is emitted downward can bounce off of the back of the chip and escape, resulting in a (2–3)× improvement in extraction efficiency. Generally, the extraction ratio does not exceed about 0.3 even for transparent substrate devices as a result of residual absorption losses at the contacts or in the active layer, or free-carrier or other types of absorption in the layers or at the chip surface.

As much as 75% of the emitted light from LEDs can come from the edges instead of the top of the LED chip. This edge light is useful for most applications since typically the LED chip is placed in a cavity that reflects the light

Table 3. Extraction ratios for encapsulated LEDs.

Epitaxial structure type	Substrate type	Emission region	Number of cones	Calculated extraction ratio[a]	Estimated actual ratio[b]	Typical device
Thin layers ($\leq 10\ \mu$m)	Absorbing	Top only	1	0.04	—	GaAsP/GaAs
Thick layers ($\geq 40\ \mu$m)	Absorbing	Top and four sides ($\sim\frac{1}{2}$ cone each)	3	0.12	0.12	AlGaAs/GaAs
Any thickness	Transparent	Top, four sides, and reflection from back surface	6	0.24	0.3	AlGaAs/AlGaAs

[a] The calculation assumes that there are no absorption losses or randomization within the chip. If randomization occurs (due to light scattering at the chip surface) the light can make multiple passes and more can escape than predicted by the calculation.

[b] These estimates are based on measured external quantum efficiency and estimated internal quantum efficiency. The internal quantum efficiency is estimated from efficiency versus temperature measurements.

in an upward direction. In some applications, such as coupling to an optical fiber or in a direct-view display, only the top-surface emission is utilized. Different light-extraction conditions pertain in this case, and a Bragg reflector as discussed in Sec. 1.7.3 may be more effective than a transparent substrate.

1.8.2 Quantum Efficiency and Power Efficiency. The external quantum efficiency is the internal quantum efficiency multiplied by the extraction ratio,

$$\eta_{ext} = R_E \eta_{int}.$$

The power efficiency (P_E) is the power output divided by the power input:

$$P_E = \frac{(\text{photons/second}) \times (\text{emission energy/photon})}{(\text{electrons/second}) \times (\text{applied voltage})} = \eta_{ext} \frac{E_R}{V},$$

where E_R is the energy of the emitted radiation.

The applied voltage is the voltage applied directly to the junction (approximately the energy gap) plus the voltage across the series (dynamic) resistance of the LED diode:

$$V \approx E_g + IR.$$

E_R is generally approximately equal to the semiconductor energy gap for near-band-edge recombination processes. The turn-on voltage for the LED is also approximately equal to the energy gap. Therefore, for low currents, where the voltage drop due to series resistance is relatively small, we have $P_E \approx \eta_{ext}$.

This approximation is accurate to within approximately 10% for most LEDs since the series resistance is typically less than 10 Ω resulting in less than a 0.2 volt increase in voltage at a typical operating current of 20 mA, while the energy gap voltage is typically 2 V.

1.8.3 Luminous Performance. For visible LEDs, the human eye is the detector, and the luminous performance, expressed in either lumens/watt or lumens/amp, is the key performance parameter.

The luminous efficiency, or the sensitivity of the eye to radiometric energy of different wavelengths, has been established by international agreement (CIE curve). The relative eye sensitivity peaks at 1.0 at a wavelength of 555 nm. At this wavelength, 1 W of radiometric power yields 680 l. The relative eye sensitivity $V(\lambda)$ drops sharply on either side of 555 nm and is about 0.5 at either 510 or 610 nm.

The luminous performance of a visible LED in units of lumens/watt is determined by multiplying the radiometric performance by the relative eye sensitivity curve, $680V(\lambda)P_E$. In some cases it is desirable to have the luminous performance expressed in lumens/ampere, which can be obtained as follows:

$$\text{luminous performance (l/A)} = 680V(\lambda)\eta_{ext} E_R.$$

1.9 Reliability

1.9.1 Radiation-Enhanced Degradation. LEDs are inherently highly reliable devices since the recombination is a normal solid-state electrical process that does not necessarily give rise to any damage to the semiconductor. However, there is a substantial amount of energy released locally (1–2 eV) with each electron–hole recombination event, and this can cause the formation or migration of point defects or dislocations, resulting in "radiation-enhanced" light output degradation. The degradation is generally accelerated by high current densities and high temperatures (Kimerling and Lang, 1975). Under extreme drive conditions (at current densities greater than $\approx$300 A/cm^2), networks of dislocations can form and grow rapidly around crystalline defects that may be present. Carriers tend to recombine nonradiatively when they are near these dislocation networks, and "dark lines" appear in the light-emitting area. Such dark-line defects (DLDs) often occur in small-emission-area AlGaAs LEDs (Fukuda, 1991) that are used as light sources for fiber-optic communications. Because the emission areas are small, extremely large current densities are common. Such devices must typically pass a "burn-in" test that verifies that they are free of the crystalline defects that lead to DLD

formation before they can be incorporated into final products.

1.9.2 Package-Related Degradation. Degradation can also be caused by the packaging methods. The encapsulating epoxy is particularly troublesome, since it has a much higher thermal coefficient of expansion than the semiconductor chip. When the LED is cooled to low temperatures, typically −20 °C or below, the epoxy contracts and substantial compressive stress is applied to the chip. When the LED is operated at low temperatures, this stress can provide a driving force for defect formation and/or migration, which results in accelerated degradation. In some cases, particularly with AlGaAs devices, DLDs can form and grow. When the LED is cooled, or temperature cycled, but not forward biased, this degradation does not occur. Another type of package-related degradation, which occurs in outdoor applications, is the discoloration of the epoxy due to ultraviolet light. The discolored epoxy absorbs some of the light emitted from the LED chip and reduces the light output of the package. Packaging-related degradation can be affected by such parameters as the proper selection of epoxy, and epoxy-curing cycles, LED chip shape, and metal reflector shape and size. Some LED materials are much more susceptible to this type of degradation than others.

1.9.3 Typical LED Degradation Characteristics. Typical LED degradation data are shown in Fig. 8. Degradation in the range of 5% to 20% is usually observed after 1000 h of operation at normal operating currents at 55 °C. The degradation generally decreases roughly linearly on a semilog plot as shown, and so the device should not reach half-brightness for more than 10^6 h. In most applications, a change in light output by less than a factor of 2 will not be noticed, and so LED reliability is generally more than adequate, particularly for indoor applications. High-performance LEDs used for outdoor applications, requiring low-temperature operation, are more susceptible to package-related degradation (Sec. 1.9.2), and must be carefully engineered to avoid nonuniform and occasionally severe degradation.

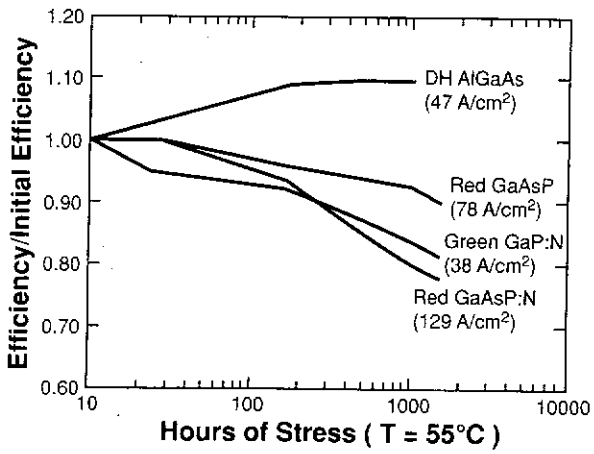

FIG. 8. Degradation data versus time are shown for several diferent types of visible LEDs at 55 °C . Most LEDs degrade by (5–20)% in light output by 1000 h, but do not fall below 50% of their initial brightness for more than 10^6 hours. The current densities shown correspond to typical drive conditions.

2. SEMICONDUCTOR MATERIALS ISSUES

2.1 Desirable Characteristics

Figure 9 shows the band gaps of various binary compounds and alloy systems plotted as a function of lattice parameter. In order to fabricate high-performance LEDs, it would be desirable to choose compounds and/or alloys from this set that have the following characteristics:

1. a direct energy gap corresponding to the emission wavelength desired,
2. higher–energy-gap materials that can be lattice matched to the active layer for the growth of injection, window, and confining layers for heterostructures,
3. a low-defect-density substrate that is lattice matched to the epitaxial structure and that is transparent to the emitted radiation,

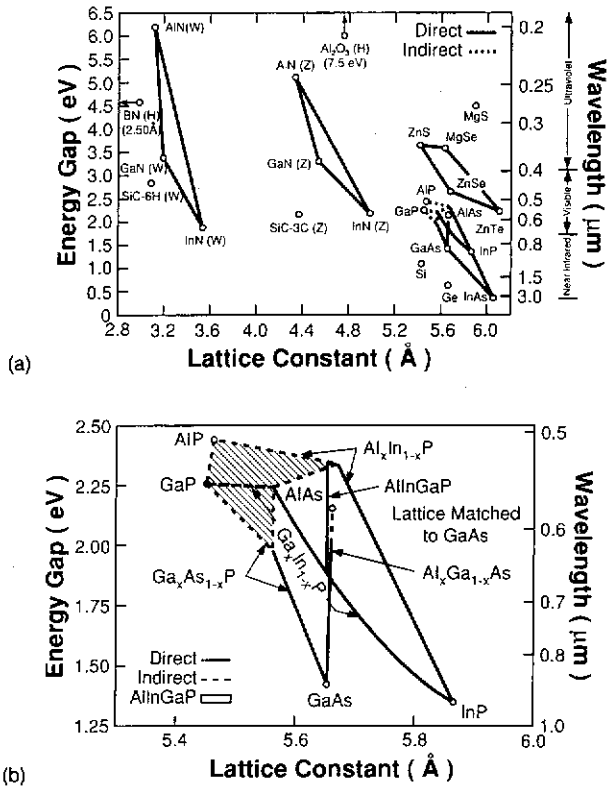

FIG. 9. (a) Energy gap vs lattice parameter for several semiconductor systems. Semiconductors that can be grown in several crystal structures are labeled Z for zincblende, W for wurtzite, and H for hexagonal. For the wurtzite and hexagonal crystals, the lattice parameter *a* is used for the lattice-constant value. (b) An enlargement of the region currently employed for most visible LEDs, showing the direct and indirect energy-gap regions.

4. the ability to add impurities to the structure to obtain a low-defect-density *p-n* junction and a low series resistance, and
5. a materials growth technology that can reproducibly and cost-effectively produce the structure as designed.

One would also like to have the lowest possible cost. Unfortunately it is not often possible to have all of these desires met simultaneously.

2.2 Energy Gap

A compound or alloy composition with an energy gap that gives the desired emission wavelength must be chosen, and, if possible, the material should have a direct energy gap. Table 4 lists energy gaps and energy-gap ranges for a variety of compounds and alloys. For infrared and red LEDs requiring energy gaps less than 2 eV, GaAs, $Al_xGa_{1-x}As$, and $GaAs_{1-x}P_x$ with appropriate compositions ($x \lesssim 0.4$) are good choices. If a compound is chosen and the energy gap is larger than desired, it may be possible to reduce the emission energy (increase the wavelength) by introducing non-band-edge recombination centers such as isoelectronic dopants. Materials with indirect band gaps and isoelectronic impurities such as GaP:N and $GaAs_{1-x}P_x$:N with $x > 0.5$ are widely used for LEDs because direct materials with energy gaps larger than about 2 eV, which are required for orange, yellow, and green LEDs, have not been available until the recent development of the AlInGaP alloy system. Materials such as ZnSe have a large enough direct band gap, but it has not been possible to form stable *p-n* junctions in ZnSe or other II-VI materials until recently.

2.3 Lattice Matching

The epitaxial layers in the device structure should, if possible, have the same lattice spacing between atoms and should match the substrate spacing as closely as possible. In other words one should try to stay on a vertical line in Fig. 9. AlGaAs and AlInGaP alloy systems grown on GaAs substrates are good examples, as is the GaInAsP system

Table 4. Materials important for LEDs.

Material system	Energy gap (eV) at 300 K	Peak emission wavelength (Å)
GaAs	1.43 direct	8670 infrared
GaP	2.26 indirect	5485 green
AlAs	2.16 indirect	5740 greenish yellow
InP	1.35 direct	9180 infrared
ZnSe	2.67 direct	4644 blue
GaN	3.39 direct	3658 ultraviolet
SiC (6*H*)	2.86 indirect	4800 blue
$GaAs_{1-x}P_x$	1.43–2.03 direct	8670–6105 infrared→red
$x_c=0.49$[a]	2.03–2.26 indirect	6105–5485 red→green
$Al_xGa_{1-x}As$	1.43–1.98 direct	8670–6525 infrared→red
$x_c=0.43$	1.98–2.14 indirect	6525–5790 red→yellow
$Ga_xIn_{1-x}P$	1.35–2.18 direct	9180–5685 infrared→yellow
$x_c=0.62$	2.18–2.26 indirect	5685–5485 yellow→green
$(Al_xGa_{1-x})_{0.5}In_{0.5}P$	1.88–2.31 direct	6596–5359 red–green
$x_c=0.70$	2.31–2.35 indirect	5359–5277 green
GaInAsP	0.724–1.35 direct	17127–9185 infrared

[a] x_c is the mole fraction at which the materials system switches from having a direct-gap band structure to an indirect-gap band structure.

grown on InP. If good lattice matching can be obtained, defects and nonradiative recombination can be minimized. It is also important to try to match the temperature coefficient of expansion because otherwise epitaxial layers that are grown lattice matched at high temperature will be strained at room temperature. If heterostructures are used, an alloy system must be chosen that allows lattice matching for alloy compositions with different energy gaps in order to permit the formation of "window" and "confining" layers without the introduction of defects at the interfaces between the layers. Some injection lasers and LEDs have been fabricated in which the active layer does not lattice match the confining layers but is so thin that it "stretches" to conform to other layers rather than creating defects. These "pseudomorphic" structures have, to date, been more effective for lasers than LEDs since the active regions must be very thin.

2.4 Substrates

Ideally the substrate should have low defect levels, be lattice matched to the epitaxial layers, and be transparent to the emitted radiation. Unfortunately, these conditions can rarely be simultaneously met. GaAs, GaP, and InP can be cost-effectively grown with reasonable levels of defects and are most commonly used. SiC and sapphire are also used in limited quantities for blue emitters. Germanium is sometimes used as a lower-cost substitute for GaAs but germanium contamination can degrade LED performance if not controlled. Silicon has also been occasionally used as a substrate for GaAs devices but the lattice match is poor and the GaAs layers are highly defective.

2.5 Dopants and Impurity Incorporation

Generally the III-V compounds, with the exception of GaN, can be easily doped either *p*-type or *n*-type so that the formation of a *p-n* junction is straightforward. Typical dopant impurities are listed in Table 5. The most common *p*-type dopant is zinc because it is

Table 5. Typical dopant impurities.

	p-type	*n*-type	Isoelectronic
III-V compounds	Zn	Te	N
	Be	Se	
	C	S	
	Mg	Si	
	Si	Ge	
II-VI compounds	Li	Al	
	Na	Cl	
	N	I	
IV compounds	B	P	
	Al	N	

safe and easy to handle, high doping levels can be achieved, and it can readily be diffused into most materials if photolithographically defined junctions are desired. Magnesium is often used in grown junctions instead of Zn since it diffuses less rapidly and is more stable in thin layer structures where dopant migration during operation could affect device performance. Carbon doping is increasingly used for similar reasons, but some materials cannot be doped *p*-type with carbon since it is a column-IV element and can be incorporated on either a column-III site where it would be *n*-type or a column-V site where it would be expected to be *p* type. Beryllium is also used as a *p*-type dopant. It can generally be incorporated in high concentrations, but it is a hazardous material to work with, and its use has been declining.

The impurity most commonly used for *n*-type doping is tellurium, although selenium and sulfur are also widely utilized. Silicon and germanium are also used for *n*-type dopants particularly for infrared applications.

Dopants that work well for infrared emitters in the direct–band-gap region may not be suitable for visible emitters in the vicinity of the direct–indirect transition. Deep donor levels associated with sulfur in GaAsP and silicon and other dopants in AlGaAs cause nonradiative transitions. One reason tellurium is so widely used for LEDs is that it has less often exhibited behavior of this type (Craford *et al.*, 1991).

Silicon carbide, which is used for blue LEDs, is a column-IV material and is generally doped with Al for *p*-type and N for *n*-type doping. Other wide–band-gap materials capable of blue emission such as GaN, and II-VI compounds such as ZnSe can easily be doped *n* type but are difficult to dope *p* type. It is only recently that it has been possible to form *p-n* junctions in these materials and to achieve blue-emitting devices. The performance and stability of these devices are not yet suitable for commercial LED applications.

3. VISIBLE EMITTERS

3.1 Materials Performance Characteristics

3.1.1 Comparison of Different Types of LEDs. The luminous performances for different types and colors of LEDs are summarized in Table 6. The AlGaAs and AlInGaP devices have the highest levels of performance and quantum efficiency. These devices satisfy most of the selection criteria discussed in Sec. 2, such as direct band gap, lattice-matched epitaxial structures and substrates, and double heterostructure device structures. At the present time, these devices are also among the most expensive and are primarily utilized only in applications requiring the maximum in performance. Lower-cost homojunction GaAsP and GaP devices dominate high-volume LED applications even though their performance is an order of magnitude lower.

3.1.2 GaAsP and GaAsP:N. $GaAs_{1-x}P_x$ LEDs were the first LEDs commercially produced, and they continue to be used in high volume since they are inexpensive and have adequate performance for many applications (Herzog *et al.*, 1969). $GaAs_{1-x}P_x$ has a direct energy gap, for $x \leqslant 0.45$, and emits in the infrared and red spectral regions. LEDs of this type have diffused homojunctions that can be photolithographically patterned, making them suitable for applications that require small emitting areas and/or more than one emitting region on each LED chip. The efficiency is relatively low because of internal absorption and a high defect density, due in part to the fact that GaAs and GaP have substantially different lattice parameters so that the GaAsP mixtures are not lattice matched to the GaAs (or GaP) substrates.

$GaAs_{1-x}P_x$, with $x \geqslant 0.45$, has an indirect band gap, and isoelectronic nitrogen must be added to achieve acceptable performance (Groves *et al.*, 1971; Craford *et al.*, 1972). The performance is still relatively low because of the indirect band gap and lattice mismatch with the GaP substrate. However, the GaP substrate is transparent, and so the extraction ratio is improved and GaAsP:N has higher luminous performance than direct–band-gap GaAsP on GaAs.

3.1.3 GaP:N, GaP:(Zn,O), and GaP. GaP:N is a green emitter with performance somewhat better than GaAsP:N. This improvement is due to a lower defect density since the GaP substrate and epitaxial layers are lattice matched (Logan *et al.*, 1968).

GaP:(Zn,O) emits in the red since the Zn and O atoms form a complex with a large binding energy (Saul *et al.*, 1969). The perfor-

Table 6. Characteristics of visible LEDs.

Table 6. Characteristics of visible LEDs.

LED type	Color (peak wavelength, nm)	Typical external quantum efficiency (%)	Typical performance (l/W)	Band-gap type	Lattice matched	Structure[a]	Substrate	Epitaxial growth method[b] (*p-n* junction formation)
$GaAs_{0.60}P_{0.40}$	Red (650)	0.2	0.15	Direct	No	Homo.	GaAs	VPE (diffusion)
GaP:(Zn,O)	Red (700)	2	0.4	Indirect	Yes	Homo.	GaP	LPE (grown)
$GaAs_{0.35}P_{0.65}$:N	Red (630)	0.7	1	Indirect	No	Homo.	GaP	VPE (diffusion)
$GaAs_{0.15}P_{0.85}$:N	Yellow (585)	0.2	1	Indirect	No	Homo.	GaP	VPE (diffusion)
GaP:N	Yellow green (565)	0.4	2.5	Indirect	Yes	Homo.	GaP	LPE (grown)
GaP	Pure green (555)	0.1	0.6	Indirect	Yes	Homo.	GaP	LPE (grown)
$Al_{0.35}Ga_{0.65}As$	Red (650)	4	2	Direct	Yes	SH	GaAs	LPE (grown)
$Al_{0.35}Ga_{0.65}As$	Red (650)	8	4	Direct	Yes	DH	GaAs	LPE (grown)
$Al_{0.35}Ga_{0.65}As$	Red (650)	16	8	Direct	Yes	DH-TS	GaAs	LPE (grown)
$(Al_{0.11}Ga_{0.89})_{0.5}P$	Orange (620)	6[c]	20[c]	Direct	Yes	DH	GaAs	MOVPE (grown)
$(Al_{0.28}Ga_{0.72})_{0.5}In_{0.5}P$	Amber (595)	5[c]	20[c]	Direct	Yes	DH	GaAs	MOVPE (grown)
$(Al_{0.43}Ga_{0.57})_{0.5}In_{0.5}P$	Yellow green (570)	1[c]	6[c]	Direct	Yes	DH	GaAs	MOVPE (grown)
SiC (6H)	Blue (480)	0.02	0.04	Indirect	Yes	Homo.	SiC	CVD (grown)
GaN	Blue (430)	0.18[d]		Direct	No	Homo.	Al_2O_3	MOVPE (grown)
$ZnS_{0.07}Se_{0.93}$	Blue green (494)	0.1[e]		Direct	Yes	DH	GaAs	MBE (grown)

[a]Homo., homojunction; SH, single heterostructure; DH, double heterostructure; DH-TS, double heterostructure with transparent, epitaxially-grown substrate (original GaAs substrate removed).
[b]VPE, vapor-phase epitaxy; LPE, liquid-phase epitaxy; MOVPE, metal-organic vapor-phase epitaxy; MBE, molecular beam epitaxy (see Sec. 5.3 for a discussion of epitaxial grown technologies).
[c]Best reported results (Huang *et al.*, 1992). Typical commercial performance not yet established.
[d]Best reported results (Nakamura *et al.*, 1991a).
[e]Best reported results (Xie *et al.*, 1992).

mance of these devices is low compared to GaP:N, even though the quantum efficiency is higher, because the eye sensitivity is an order of magnitude lower for the 700-nm GaP:(Zn,O) emission than that for the green GaP:N emission.

Green-emitting LEDs can also be constructed in GaP without nitrogen doping. These devices depend upon phonons to conserve momentum (see Sec. 1.3). The absence of the nitrogen recombination center increases the radiative lifetime by about an order of magnitude. This reduces the quantum efficiency, but, since the absence of nitrogen also improves the crystal quality somewhat so that the nonradiative lifetime is also increased, the quantum efficiency is only (3–4)× lower than that for GaP:N. GaP devices also have an advantage in that the emission is greener (555 nm vs 565 nm) since the nitrogen trap is not involved.

3.1.4 $Al_xGa_{1-x}As$. The $Al_xGa_{1-x}As$ material system has a direct energy gap for compositions $x \leqslant 0.4$ and can be used to produce highly efficient red and infrared emitters. Since AlAs and GaAs have nearly the same lattice parameters, the system is well matched to GaAs substrates, so that defects can be minimized and heterostructures of various types can be grown (Nishizawa and Suto, 1977; Cook *et al.*, 1988). Three types are commercially available: single heterostructure on a GaAs substrate, double heterostructure on a GaAs substrate, and a double heterostructure with a thick confining layer and the GaAs substrate removed.

As indicated in Table 6, the performance increases as the structural complexity increases primarily because of reduced absorption as discussed in Sec. 1.7. The cost also increases with complexity, and so all three types of AlGaAs structures are utilized depending upon the price-performance trade-off desired.

Visible AlGaAs LEDs are produced by liquid-phase epitaxy (see Sec. 5.3.2). This is a mature technology that is also used for GaP LEDs. However, the growth of the multilayer AlGaAs heterostructures, particularly with thin 1–3-μm-thick active regions and ultrathick (>100 μm) confining layers, requires substantially more complex growth equipment than that used for the relatively simple GaP devices.

3.1.5 AlInGaP. The AlInGaP material system has a direct–indirect crossover in the green spectral region at an estimated energy of 2.31 eV (Cao and Stringfellow, 1990). It is the only system in which lattice-matched direct-band-gap heterostructures for colors other than infrared and red can be readily fabricated at this time. Lattice matching requires that the indium concentration be kept equal to the sum of the Al and Ga compositions since InP and GaP have lattice parameters about equal distances on opposite sides of that of the GaAs substrate (see Fig. 9). The ratio of Al to Ga can be changed to form heterostructures since Al and Ga are the same size atoms. Other wide-band-gap materials are beginning to show promise but are not yet commercially viable.

The three types of AlInGaP structures grown are shown in Fig. 10. All consist of double heterostructures on a GaAs substrate. The top window or spreading layer is grown relatively thick (~ 50 μm) to maximize the extraction of light from the edge of the chip (see Sec. 1.8.1).

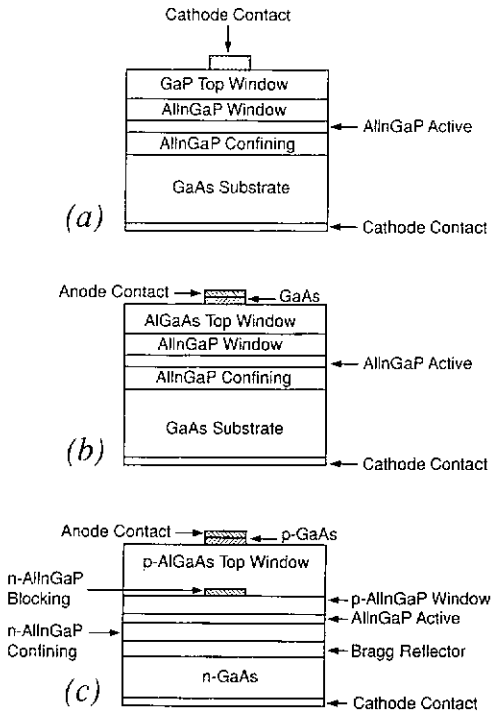

FIG. 10. Cross section of AlInGaP chip structures: (a) GaP window layer, (b) AlGaAs window layer, and (c) AlGaAs window layer with a blocking layer beneath the top contact and a Bragg reflector beneath the active layer.

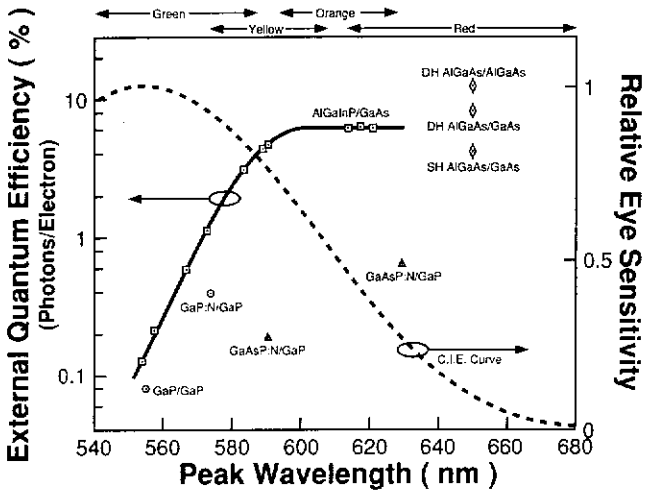

FIG. 11. AlInGaP quantum efficiency as a function of wavelength compared to other LED technologies. For red and yellow wavelengths beyond 590 nm, the devices have 5% external efficiency into air. The efficiency drops at shorter wavelengths as a result of the approaching transition from a direct to an indirect semiconductor. SH stands for single heterostructure and DH stands for double heterostructure. The CIE eye-response curve is also shown. Reprinted from Craford (1992), courtesy of the Institute of Electrical and Electronics Engineers, Inc. Copyright © 1992 IEEE.

The top window layer could, in principle, be grown of AlInGaP; but AlInGaP has a high resistivity and is costly to grow, and so AlGaAs and GaP have generally been substituted (Kuo *et al.*, 1990; Fletcher *et al.*, 1991; Sugawara *et al.*, 1991; Huang *et al.*, 1992). AlGaAs has the advantage that it is lattice matched but the disadvantage that it absorbs some of the light in the case of yellow and green emitters. GaP is transparent and inexpensive, but it is not lattice matched. This does not appear to introduce defects in the active region since the GaP layer is the last layer grown, and the best results, to date, have been obtained with a GaP window.

The quantum efficiency and luminous performance of AlInGaP devices compared to other types of LEDs are shown in Figs. 11 and 12, respectively. The external quantum efficiency for wavelengths greater than 590 nm is about 5% but falls rapidly for shorter wavelengths as the direct-indirect transition is approached. The luminous performance peaks in the region of 590 nm and falls on both sides as a result of changes in both the eye sensitivity (also shown in Fig. 11) and internal efficiency.

AlInGaP devices are clearly superior to any other technology from 590 to 620 nm and can be expected to continue to improve since the

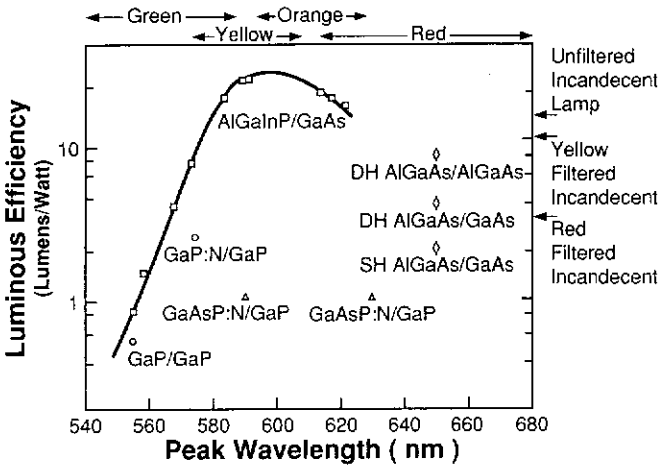

FIG. 12. LED luminous performance vs wavelength for AlInGaP compared to other LED technologies. Luminous performance is the product of power efficiency (roughly equal to quantum efficiency) and the eye's response. Reprinted from Craford (1992), courtesy of the Institute of Electrical and Electronics Engineers, Inc. Copyright © 1992 IEEE.

technology has only recently been introduced. It is reasonable to expect that AlInGaP devices will have superior performance for all wavelengths from ~550 to ~630 nm in the future and should even surpass AlGaAs at 650 nm if transparent-substrate devices can be developed.

AlInGaP is grown using the metal-organic vapor-phase epitaxy technique (see Sec. 5.3.4), which is still evolving as a production technology. As a consequence, these devices are now relatively expensive but can be expected to decrease rapidly in cost as the technology is refined.

3.1.6 GaN. GaN has a direct energy gap of 3.4 eV, which is suitable for blue LEDs, but there are two problems that have limited the application of GaN. There is no substrate that provides a good lattice match, and it is difficult to form *p-n* junctions.

The most commonly used substrate is sapphire (Al_2O_3). Sapphire is transparent, which is good, but is so poorly matched both structurally and thermally that the defect density is high. Other materials such as SiC, MgO, and ZnO are being investigated.

GaN is generally *n* type as grown, probably as a result of nitrogen vacancies. It has been extremely difficult to produce high-quality *p*-type GaN. Recently GaN doped with Mg has been converted to *p*-type through the use of electron-beam irradiation, and *p-n* junctions have been formed (Nakamura *et al.*, 1991b; Amano *et al.*, 1990). If this process can be commercialized, low-voltage GaN devices should become available. At the present time GaN devices are generally higher-voltage metal–insulator–semiconductor devices.

In the future, the AlInGaN material system can be expected to be developed. Since AlN has an energy gap of 6.2 eV, devices with wavelengths ranging into the ultraviolet should become possible.

3.1.7 ZnSe. Materials from columns II and VI of the periodic chart, such as ZnS and ZnSe mixtures, have direct energy gaps exceeding 2.5 eV and are also suitable for blue LEDs. These materials can be lattice matched to GaAs substrates, which is a major advantage compared to GaN. However, *p-n* junctions have also been difficult to form in ZnSe. Recently, nitrogen doping has been used to produce *p*-type material and to fabricate injection lasers and LEDs emitting in the blue-green spectral region (Haase *et al.*, 1991; Jeon *et al.*, 1992). These devices are promising but have had reliability problems. At the time of this writing, it is not clear whether these are fundamental limitations or if they can be improved to yield satisfactory commercial emitters.

3.1.8 SiC. Silicon carbide is a column-IV material with an indirect energy gap of 2.86 eV. It is the most widely utilized type of blue emitter at this time (Edmond *et al.*, 1992). Devices are formed by growing a SiC epitaxial film on a SiC substrate using either MOVPE or LPE. *p-n* junctions can be readily obtained by doping with Al for *p*-type and N for *n*-type material. The efficiency is relatively low because of the indirect band gap. The light output has been steadily improving as the materials growth technology is refined and, if a suitable isoelectronic impurity can be found, as in the case of GaP:N, it may be possible to improve the light output significantly.

3.2 Operating Characteristics

3.2.1 Current–Voltage Characteristics. Turn-on voltages for LEDs typically range from about 1.5 V for red devices to more than 5 V for blue devices depending upon the material system and whether or not a *p-n* junction can be formed. Some typical current–voltage characteristics are shown in Fig. 13.

The operating current for visible LEDs can range from 1 mA or less for indicator applications to 100 mA or more for illumination applications such as automotive exterior lighting. The operating voltage is the sum of the voltage at the junction plus the voltage due to the product of the forward current and the device dynamic resistance. The dynamic resistance will be higher if the LED chip is smaller in area, thicker, or made of less-conductive (more lightly doped and/or lower-mobility) material. Unfortunately, it is often desirable to use small chips to reduce cost, thick chips to get efficient light extraction from the edges, and lightly doped material to minimize nonradiative recombination. These conflicting requirements result in different optimal LED chip designs for different applications.

The reverse breakdown voltage is generally limited by avalanche breakdown in the *n*-type

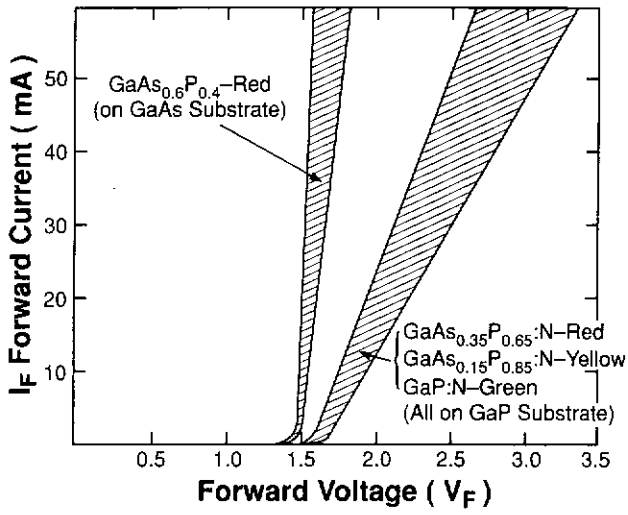

FIG. 13. Typical current-voltage characteristics for red-, yellow-, and green-emitting LEDs. The red-emitting $GaAs_{0.6}P_{0.4}$ on GaAs substrate has a typical dynamic resistance of 2–6 Ω. The nitrogen-doped devices on GaP substrates have typical dynamic resistances of 20–30 Ω. Reprinted from Tannas (1985), courtesy of Van Nostrand Reinhold Company, Inc. Copyright © 1985.

region of the LED, which is determined by the carrier concentration. In some double heterostructure devices, reverse breakdown can also occur as a result of "punch through" when the depletion region reaches an interface. In either case, the reverse breakdown voltage is generally substantially more than 10 V for visible LEDs. This is large enough for most applications, and breakdown voltage is generally not an issue as long as a high-quality *p-n* junction is utilized and reverse-current leakage is minimized.

3.2.2 Performance versus Current. The LED performance shown in Table 6 corresponds to a typical operating current in the range of 20 mA. LED performance will change with current (or current density) depending upon a variety of factors such as the concentration of nonradiative centers in the vicinity of the junction and heating due to both nonradiative recombination and Joule heating associated with the dynamic resistance. Typically LED efficiency will go through three stages—superlinear, linear, and sublinear—as a function of increasing current. This is illustrated in Fig. 14.

At low currents, the light output is superlinear, since nonradiative centers provide a shunt path that saturates as the current density increases. GaAsP devices with high defect densities typically show more superlinearity than AlGaAs devices, which are lattice matched and have low defect densities.

At moderate current densities the light output remains linear with current (and the efficiency is constant). At higher current densities, heating causes the efficiency to drop and the light output becomes sublinear with

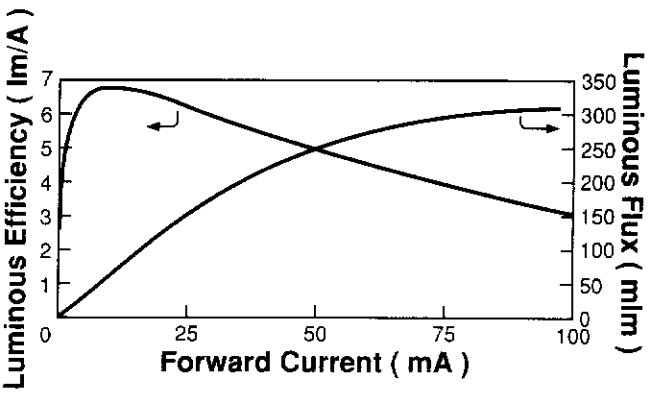

FIG. 14. Efficiency and light output as a function of d.c. current for a double-heterostructure AlGaAs LED. At low currents, the light output is superlinear. From 5 to 20 mA the light output is a linear function of current, and above 20 mA, the light output becomes sublinear because of heating effects.

current and will eventually decrease with increasing current as the heating becomes severe.

For most LEDs the light output drops at the rate of between 0.5% and 2% per degree centigrade measured at the junction. This rise in temperature of the *p-n* junction can be estimated in a given application if thermal resistance (the ratio of the steady-state rise in temperature to the power applied) for a given package is known. The thermal resistance of a typical LED lamp is 220 °C/W.

3.3 Applications

3.3.1 Overview. Traditionally, visible LEDs have been used for indicators on instruments, computers, and consumer electrical equipment. LEDs are used in the form of discrete LED lamps, numeric displays, or alphanumeric displays. These applications are particularly cost-sensitive and are dominated by lower-cost and -performance LED technologies. Emerging LED markets such as outdoor large-area displays and exterior lighting for automobiles often require LEDs with the maximum possible performance and, in addition, require devices that are robust when operated in outdoor environments. Visible LED applications are summarized in Table 7.

3.3.2 Instrument and Computer. In these markets LEDs are used both as discrete indicator lamps and as numeric and alphanumeric displays. Most of these applications are not battery powered, and traditional LED performance (~1 l/W) is often adequate. However, operation at low currents so that the LEDs can be driven directly from integrated circuits can be important, and may require higher-performance devices. Reliability is a key concern in these markets, and this gives LEDs an important advantage. Cost pressure from competitive technologies such as liquid-crystal displays is severe, particularly for numeric and alphanumeric display applications. LEDs are often used to backlight liquid-crystal displays, and for this purpose higher-performance LEDs are often utilized.

Surface-mounted LED packages have become increasingly important as LED users automate their processes in order to improve quality and reduce cost.

3.3.3 Consumer Electronics. These markets also generally use LEDs in the form of either discrete lamps or numeric displays. Applications include audio equipment, home appliances, clocks, radios, TV-channel tuning, toys, etc. This is a very-high-volume market and cost is the most critical issue. Standard lower-performance LED technologies are generally utilized. For many of these applications, the oldest and lowest-performance LED technologies [red GaAsP and GaP:(Zn,O)] are widely utilized.

3.3.4 Large-Area Display. The large-area display market has been growing rapidly. These displays can be "electronic billboards" as large as several meters high and wide, or as small as several inches high and wide. Some applications are outdoors, in which case high-performance LED technologies are required to provide sunlight viewability.

Indoor applications generally utilize the lower-performance technologies, often using red GaAsP:N and green GaP:N devices in

Table 7. Main technologies for different applications. Key: ●, primary technology; ◑, secondary technology; ○, potentially important.

Application area	Technology: Red GaAsP/GaAs	Red GaP:(Zn,O)	Red, yellow, orange GaAsP:N	Green GaP:N	Red AlGaAs	Yellow, orange AlInGaP	Blue SiC
Consumer	●	●	●	●	◑		
Industrial	◑	◑	●	●	◑	○	
Automotive							
Interior			●	●		○	
Exterior					●	○	
Large-area displays							
Interior			●	●	◑	○	○
Exterior			◑	●	●	○	
Electrophotographic	●						

pairs. By adjusting the drive current to the two LEDs, the perceived color can be changed from red to green. Blue is required to achieve full-color displays, and this is one of the major potential markets for the emerging blue technology.

The high-brightness red, orange, and yellow-amber AlInGaP and AlGaAs technologies are generally used outdoors. Electronic highway signs, where amber is generally desired, and advertising signs, where any color can be used, are among the applications.

3.3.5 Vehicular Lighting. LEDs are increasingly popular in and on vehicles because of their reliability and ruggedness as well as for styling reasons. LEDs are small and thin and do not burn out. AlGaAs and AlInGaP LEDs are incorporated in automobile trunks and "spoilers" to serve as brake lights, and they are being used on trucks and automobiles as side markers and "running lights."

LEDs are also used as indicator and display devices on the interior of vehicles. Dashboard displays generally use the GaAsP:N and GaP:N technologies, although higher-performance technologies are sometimes used to backlight liquid crystal displays.

3.3.6 Electrophotography. LEDs are generally used in electrophotographic equipment either to "write" or to "erase" a message on a revolving photoconductive drum. The LEDs are configured in a thin bar as long as the paper is wide. The drum picks up toner in selected areas determined by the LED "write" function and deposits the toner on the paper.

The LED "write bar" consists of an array of several thousand LEDs with a linear density of typically 300/in. The arrays typically consist of a series of red-emitting GaAsP monolithic chips, where each chip has 64 or 96 2–3-mil-diam junctions in a row. The drum is then "erased" by light from the LED "erase bar." The LED erase bar is a lower-resolution linear array, and discrete AlGaAs LED chips are commonly employed.

LED "write bars" compete with laser printers and at this time have a small share of the market. LEDs can provide very high-speed, high-quality printing, but the cost of LED printers is generally higher than that of laser printers.

3.3.7 Trends and Future Developments. Visible-LED markets will grow and new applications will emerge as electronics becomes increasingly pervasive. The standard LED technologies will continue to be used for applications where their light output is adequate. The higher-performance technologies will decrease in cost and will be used where high light output or low drive currents are important. Large-area displays and vehicular lighting are expected to become large markets. The development of a high-performance blue technology should occur, which would make full-color large-area displays possible and help the outdoor large-area–display market to grow rapidly.

4. INFRARED EMITTERS

4.1 Materials Performance Characteristics

4.1.1 Comparison of Different Types of Infrared LEDs. The detectors used for infrared LEDs are photodiodes or phototransistors instead of the human eye. The radiometric power output of the LED is therefore a key performance parameter. The rate at which data can be transmitted is determined in part by the LED switching speed, and this is also an important performance parameter for IR LEDs (one that is totally unimportant for most visible applications). A summary of performance characteristics for several types of IR emitters is shown in Table 8.

4.1.2 GaAs:Zn. The first IR emitters available were diffused-junction devices similar to the $GaAs_{1-x}P_x$ LEDs described in Sec. 3.1.2 (Keyes and Quist, 1962). There is a similar trade-off (Herzog *et al.*, 1972) between avoiding surface recombination problems (deep junction optimal) and reducing internal absorption (shallow junction optimal). Because of their low power output, they are no longer extensively used.

4.1.3 GaAs:Si and AlGaAs:Si. At liquid-phase epitaxial (LPE) growth temperatures > 820 °C, Si incorporates as an *n*-type dopant in both GaAs and AlGaAs, while at lower temperatures it incorporates as a *p*-type dopant. By simply cooling a GaAs or AlGaAs melt on a GaAs substrate through this temperature, a *p-n* junction can be grown. The dominant

Table 8. Characteristics of IR LEDs.

LED type	Wavelength (nm)	External quantum efficiency (%)	Typical performance output power[a] (mW at 50 mA)	90% to 10% fall time (ns)	Device[b] structure	Substrate	Epitaxial growth method (*p-n* junction formation)
GaAs:Zn	900	3–4	2–3	50	Homo.	GaAs	BG[c] (diffusion)
GaAs:Si	940	9–14	6–9	1000	Homo.	GaAs	LPE (grown)
AlGaAs:Si	880	11–18	8–13	500	Homo.	GaAs	LPE (grown)
AlGaAs	780–880	4–6	3–5	20–40	SH	GaAs	LPE (grown)
AlGaAs	780–880	10–14	7–10	20–40	DH	GaAs	LPE (grown)
AlGaAs	780–880	20–27	15–20	20–40	DH-TS	GaAs	LPE (grown)
SEA[d] AlGaAs	820–880	—	—	4–15	DH	GaAs	LPE/MOVPE (grown/diffusion)
SEA[d] InGaAsP	1300–1500	—	—	≈2.5	DH	InP	LPE/MOVPE (grown)

[a]Encapsulated lamp form.
[b]See Table 6 for definitions.
[c]Horizontal Bridgeman.
[d]SEA stands for small emission area.

recombination process that occurs is between donor and acceptor band-tail states, and sub-band-gap light is generated. The rest of the crystal is fairly transparent to the light generated in GaAs:Si LEDs, and thus they have high output efficiencies (Rupprecht *et al.*, 1966). In AlGaAs:Si LEDs, the GaAs substrate is typically removed (see Fig. 15), and the device is processed "*n*-side-up" to reduce internal absorption (Dawson, 1977). This donor-acceptor recombination process is, however, quite slow ($\approx 1\ \mu s$), and such LEDs cannot be used in data communication applications at frequencies greater than several hundred kilohertz. Nonetheless, because of their high output power and low cost, they continue to be used extensively as the light sources in remote controls for televisions and VCRs.

4.1.4 $Al_xGa_{1-x}As$. As was mentioned for the visible emitters (Sec. 3.1.4), the small variation in lattice parameter from GaAs to AlAs has made possible the growth of very high-quality heterostructure devices in the $Al_xGa_{1-x}As$ materials system. Single-heterostructure, double-heterostructure, and "transparent-substrate" double-heterostructure emitters are also available in the infrared portion of the spectrum. The internal efficiency of these devices is near 100% (Alferov *et al.*,

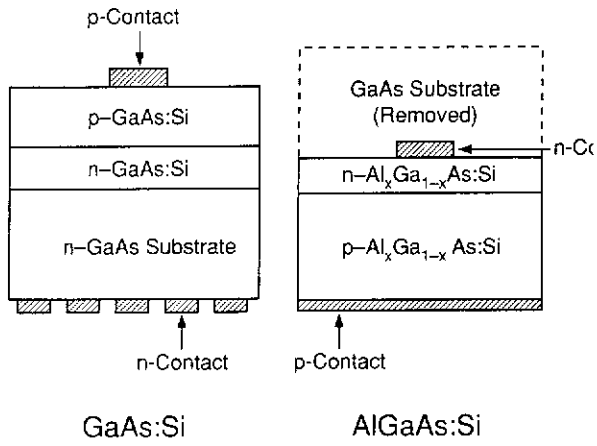

FIG. 15. Chip structures of GaAs:Si and AlGaAs:Si infrared emitters. Both the *p*-type and *n*-type epitaxial layers are grown by LPE from a single melt. In AlGaAs:Si emitters, the original GaAs substrate is removed (to reduce absorption) and the device is processed "*n*-side up".

1975) and does not vary much as the emission wavelength is changed from ~700 nm to 880 nm. High-quality devices can be grown in this wavelength region by both MOVPE and LPE. However, the thick layers necessary for efficient optical extraction are most easily grown by LPE. Double-heterostructure transparent-substrate AlGaAs emitters provide more power output than any other type of infrared LED and are roughly 20 times faster than Si-doped GaAs and AlGaAs emitters. Their use will continue to expand as more efficient manufacturing processes are developed and their cost decreases.

4.1.5 Small-Emission-Area AlGaAs and InGaAsP. Most of the IR LED emitters described above are unsuitable for fiber-optic data-communication applications as they are too slow, and it is difficult to couple the emitted light efficiently into the small ($\approx$60 μm diameter for multimode and $\approx$7 μm diameter single-mode) fiber cores. To improve performance in both of these areas, the emission area is typically reduced. The resultant increased current density shortens the lifetime, and the smaller emission area is easier to focus into the fiber core. This reduction in emission area is accomplished by either introducing current-blocking layers into the structure, etching mesas, or switching to a "stripe" geometry and forming an edge emitter (see Saul *et al.*, 1985; Pearsall, 1982). The power that can be coupled into a fiber is the important performance parameter for these devices and no values are listed in Table 8 for total output power.

The wavelength of these emitters is chosen to match regions of minimum attenuation in optical fiber. The first minimum occurs at ~850 nm and AlGaAs emitters are used. Two other minima occur near 1300 and 1550 nm, and InGaAsP emitters are used.

4.2 Operating Characteristics

4.2.1 Current-Voltage Characteristics. As with the visible LEDs, the turn-on voltage of infrared LEDs varies with the band gap of the material. InGaAsP emitters have turn-on voltages of ~0.8 V while GaAs:Si and AlGaAs emitters have turn-on voltages of 1.2 V. The operating current varies dramatically depending upon the application. Some small-emission-area AlGaAs LEDs used in data-communication applications can be driven at currents as low as 10 mA, while GaAs:Si emitters used in remote-control applications are pulsed up to 1.5 A. Large chips ($400\times400\ \mu m^2$) are used in the high-current devices to reduce both the thermal and the dynamic resistances of the device. To keep the total forward voltage below 3.0 V (two 1.5-V batteries in series) at a current of 1.5 A, the dynamic resistance of the LED must be kept below ~1 Ω.

Again, as with the visible LEDs, the reverse breakdown voltage is limited by avalanche breakdown and is determined by the doping level on the most lightly doped side of the *p-n* junction. As the infrared emitters are usually more heavily doped than visible emitters, their breakdown voltages are typically lower, in the 7–60-V range.

4.3 Applications for Infrared Emitters

4.3.1 Remote Controls. As was mentioned above, one of the highest-volume applications for IR LEDs is for remote controls that are used in televisions, audio equipment, and VCRs. Here the information is sent from the remote control through the air in a sequence of pulses and a high-sensitivity Si *p-i-n* detector is used as the receiver. The higher the LED output power, the further one can be from the receiver and still have it work. The amount of data to be transmitted, however, is quite small, and slow GaAs:Si or AlGaAs:Si emitters are sufficient. These LEDs are driven at currents up to 1.5 A in order to maximize the transmitter–receiver distance.

4.3.2 Optocouplers. If the emitter and detector are placed opposite each other inside a light-shielded package [see Fig. 16(a)], signals can be "coupled" from one electrical circuit to another without an electrical connection. Devices of this type are called optocouplers and can be used to provide electrical isolation of up to 5 kV. They are used to isolate high- and low-voltage circuits and to eliminate interference problems. GaAs:Si, AlGaAs:Si, visible GaAsP, and AlGaAs emitters are all used in optocoupler applications depending upon the speed–power–cost trade-off desired.

4.3.3 Sensors. If there is an optically accessible path between an emitter and a detector, the presence or absence of an object in that path can be sensed. A typical example is the slot interrupter shown in Fig. 16(b) in

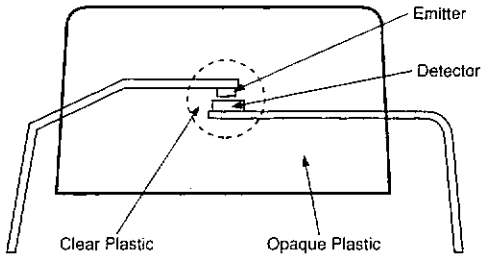

(*a*) **Optocoupler**

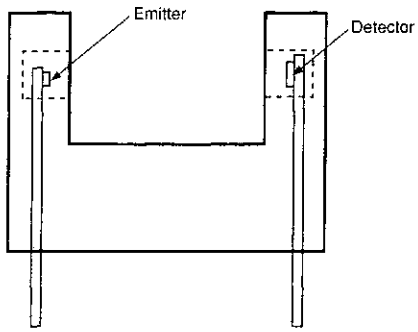

(*b*) **Slot Interrupter**

FIG. 16. (a) Optocoupler and (b) slot interrupter configurations for emitter–detector pairs. The emitter and detector in an optocoupler are shielded from external light sources by opaque plastic while the optical path is accessible in a slot interrupter. An object passing between the emitter and detector in a slot interrupter blocks the optical path and can therefore be sensed.

which an emitter and detector face each other across the opening of a U-shaped plastic holder. If an object passes between the emitter and detector, the optical path is blocked and a signal is generated. Typical applications for slot interrupters are to count objects, to sense paper in a copier, and to check for the write-protection sticker on a floppy disk.

Such sensors can also be configured to work in a reflective mode where the emitter and detector are positioned close to each other and face the same direction. If a reflective surface passes in front of them, light from the emitter is reflected to the detector and is sensed.

4.3.4 Optical Communications (*q.v.*). As was mentioned in Sec. 4.1.5, LEDs with small emission areas that can be effectively coupled into optical fibers have been developed and are the emitters of choice for data rates below 200 Mbd and distances shorter than ~8 km. For higher data rates and longer distances, laser diodes are used. The wavelength of the emitter is chosen to correspond to one of the several minima in the absorption of optical fiber. One minimum occurs at ~850 nm and AlGaAs emitters are used. Two other minima occur at 1300 and 1550 nm and InGaAsP emitters are used.

4.3.5 Trends and Future Developments. The remote-control and sensor markets are fairly mature and are not expected to grow rapidly. Data-communications applications will continue to grow as more and more Cu wire is replaced by optical fiber. Through-the-air data-communication applications such as wireless sound transmission from a television to headphones or from a personal computer to a printer are also expected to grow rapidly. These applications require both high power and high speed, and thus double-heterostructure transparent-substrate AlGaAs emitters are the best choice.

5. TECHNOLOGY

5.1 Overview

LED production technology consists of several basic steps: substrate growth, epitaxial growth, and wafer fabrication into finished components. LED technology is similar in many ways to the technology utilized to fabricate silicon integrated circuits. However, the materials used to fabricate LEDs are much more complex than elemental silicon and are more difficult to produce and process. As a consequence, the evolution of compound-semiconductor technology is far behind silicon in terms of the size of crystals grown, defect densities, volumes of device produced, and automation and cost reduction.

5.2 Substrate Growth

The most common LED substrates are GaAs, GaP, and InP. They are generally grown using the liquid-encapsulated Czochralski (LEC) technique. This technique is an extension of the Czochralski technique used to grow silicon crystals (see CRYSTAL GROWTH). A single-crystal "seed" is dipped into a molten solution

of the material to be grown and, as the seed is pulled from the melt and cooled, a single crystal forms on the end. Liquid encapsulation, which is a layer of boric oxide on top of the melt, is required to keep the volatile As and P from vaporizing from the melt. The crystal growth occurs above atmospheric pressure so that the boric oxide will stay in place on top of the melt.

Typically crystals 2 and 3 in. in diameter and less than 12 in. long are grown. These crystals are then sliced into wafers 15 to 20 mils thick that are used as the substrates for the epitaxial films.

5.3 Epitaxial Growth

5.3.1 Epitaxial Growth Overview. There are four technologies used for the growth of the epitaxial films; liquid-phase epitaxy (LPE), vapor-phase epitaxy (VPE), metal-organic vapor-phase epitaxy (MOVPE), and molecular-beam epitaxy (MBE). LPE and VPE are well-established high-volume technologies used to grow GaAsP, GaP, and AlGaAs, which dominate the production of LEDs at this time. MOVPE is generally used for the growth of AlInGaP and other quaternary materials and is emerging as a LED production technology. MBE is not widely used for LED production at this time but is the only epitaxial technology that has been successfully used to produce *p-n* junctions in ZnSe. Thus, if ZnSe becomes the technology of choice for blue emitters, MBE could become an important LED growth technology.

5.3.2 Liquid-Phase Epitaxy. LPE is the highest-volume LED technology. It is used for the growth of various types of GaP, GaAs, and AlGaAs LEDs. The LPE process consists of placing a molten solution (hence the name LPE) of Ga, which is saturated with the material to be grown, in contact with the substrate wafer at high temperature (generally 600–900 °C). As the solution is cooled, an epitaxial film is formed on the substrate wafer. Successive layers with different compositions or doping types can be grown by sliding the substrate wafer from one Ga melt to another. The growth apparatus consists of graphite chambers that hold the melts and substrates and facilitate transferring the substrates from one melt to another.

The LPE technique has the advantage that it is relatively easy to grow high-quality layers. However, it becomes more complicated as the number of wafers and layers to be grown increases, and it is not suitable for the controlled growth of complex structures with layer thickness much less than a micrometer thick.

5.3.3 Vapor-Phase Epitaxy. VPE is a high-volume technology that is primarily used to grow GaAsP and GaAsP:N layers. The substrate wafers are placed in the coolest part of a heated growth chamber and the material to be grown is transported to the surface of the wafer in gaseous form (hence the name VPE) and deposited upon the relatively cool substrates [see CVD (CHEMICAL VAPOR DEPOSITION)]. The gases consist of PH_3, AsH_3, and gallium chlorides that are formed by passing HCl over Ga metal. Hydrogen and dopant gases are also present. The VPE technique has the advantages that large numbers of wafers can easily be grown upon simultaneously, and the layer composition can be readily changed as frequently as desired simply by changing the gas composition during growth. VPE has the disadvantage that AlGaAs and AlInGaP cannot be grown because the aluminum-bearing gases tend to attack the hot quartz walls of the chamber and contaminate the epitaxial films. This limitation is not present in MOVPE.

5.3.4 Metal-Organic Vapor-Phase Epitaxy. MOVPE (*q.v.*) is similar to VPE except that metal-organic gases such as trimethylgallium (TMG) are used to transport the growth metals, and the growth reaction is pyrolytic so that the substrate wafer is in hottest part of the growth chamber and the walls of the chamber can stay relatively cool. This minimizes the reactions of the growth gases with the walls and enables aluminum-containing compounds to be grown.

5.3.5 Molecular-Beam Epitaxy. MBE (*q.v.*) is a high-vacuum technology. The substrate wafers are placed in a special vacuum chamber and held at an appropriate growth temperature. The growth materials are then evaporated from controlled source ovens. MBE can grow extremely thin layers and complex structures with a high degree of control. It has not been used for cost-effective high-volume production of LEDs. If MBE is needed to

produce high-performance ZnSe blue LEDs, high-volume production capability will have to be developed.

5.4 Wafer Fabrication

5.4.1 Junction Formation. Generally the *p-n* junction is formed during the epitaxial growth step. However, for GaAsP and some other types of devices this is not done. In this case, *p-n* junction diffusion is the first step in wafer fabrication. The junction is generally formed by the diffusion of zinc into the crystal. If a patterned junction or a monolithic chip with several junctions is required, a silicon nitride (Si_3N_4) film is first deposited and then holes are opened in the Si_3N_4 to determine where the Zn will diffuse. The diffusions are carried out in ampoules at temperatures from 600 to 900 °C for times ranging from minutes to hours.

5.4.2 Ohmic Contact Formation. If the *p-n* junction is formed during the epitaxial growth step, as is generally the case, wafer fabrication consists primarily of the formation of Ohmic contacts on the wafers. The Ohmic contact consists of patterned metal films, which may have several layers. Ohmic contacts are formed using evaporation, *e*-beam, or sputtering depending upon the contact metals. Typical *p*-type contacts contain alloys of Au-Zn or Au-Be. The *n*-type contacts typically use materials such as Au-Ge alloys. The contact materials are deposited on the epitaxial wafers and then heated to typically about 400 °C to form a low-resistance Ohmic contact.

Multilayer contacts are often employed because the surface of the contact must be suitable for high-speed wire bonding. This requires a relatively pure Au or Al film with a minimum of oxides that can form if Ga or other materials diffuse to the surface. Consequently a barrier layer of W or similar material is often deposited on top of the contact followed by the deposition of a final Au or Al layer. The contacts may be patterned using photolithographic techniques or by carrying out the depositions through metal masks.

5.4.3 Dicing. After the wafer fabrication is complete, the wafers are separated into chips. In some cases the wafers are tested for optical and electrical performance before dicing. Dicing is generally accomplished with a dicing saw, which uses a thin circular diamond-impregnated blade. Sometimes chips are scribed and broken, but the chip quality is better with a dicing saw. The wafer is placed on an elastomer tape before sawing, and the chips remain on the tape until they are die-attached. The tape is usually expanded, separating the chips further apart, before die attachment.

5.5 Assembly

5.5.1 Die Attachment. The LED chips are removed from the tape used in sawing or scribing and placed in position in the device assembly by high-speed die-attachment machines that operate at rates in excess of 3000 chips/h. These machines first deposit a drop of conductive epoxy and then place the chip in the epoxy. Following die attachment, the epoxy must be cured prior to wire bonding. Depending upon the final device type, the chips may be attached to a metal lead frame, a printed circuit board, or a ceramic substrate.

5.5.2 Wire Bonding. The wire bonding is also done by high-speed machines that can perform more than 3000 bonds/h. They use heat and pressure (thermocompression bonding) and/or scrubbing (ultrasonic bonding) to achieve a bond. The bonding wires are typically 1 mil thick and are gold or aluminum. Wire bonding is important in determining device reliability, and the quality of the metal bonding pad on the LED chip and process control in the bonding operation are critical. If the integrity of the bond is not good, the wire can pull off during encapsulation or when the device is in operation, particularly during temperature cycling. If the bonding process is too severe, the LED chips, which are quite fragile, can be cracked, which also causes reliability problems.

5.5.3 Encapsulation. Most LED devices are encapsulated in some type of polymer, generally epoxy. The epoxy serves to match the index of refraction better (see Sec. 1.8.1) so that more light is extracted, as a lens to focus the light in the desired radiation pattern, and as a structural medium to hold the package together and protect the fragile wire-bonded LED. However, the epoxy has a much higher coefficient of expansion than the LED

chip, and so during operation and temperature cycling, it can cause stress and damage the chip instead of protecting it. In the case of integrated circuits and most other electronic devices, the encapsulating polymers are "filled" with graphite fiber or some other material that reduces the expansion coefficient. However, since LEDs must emit light, opaque filler cannot be used, and the selection and curing of the epoxy encapsulant are critical reliability issues. This is particularly true for exterior application where large temperature extremes are experienced.

The encapsulation epoxy may be completely clear so that the light can be focused in a narrow beam, or may have a small amount of diffusant, such as glass particles, added to spread the light if wide-angle viewing is desired. The epoxy may also be tinted to match the color of the LED.

The encapsulation is usually done by casting, although transfer molding is sometimes used. Injection molding has not been widely used because the polymers that can be injection molded have not been compatible with LED reliability requirements.

List of Works Cited

Alfërov, Zh. I., Chikovani, R. I., Charmakadze, R. A., Mirianashvili, G. M., Zosimov, N. K., Grigoryan, N. A. (1973), *Sov. Phys. Semicond.* **6**, 1930–1931.

Alfërov, Zh. I., Andreev, V. M., Garbuzov, D. Z., Rumyantsev, V. D. (1975), *Sov. Phys. Semicond.* **9**, 305–309.

Amano, H., Asahi, T., Akasaki, I. (1990), *Jpn. J. Appl. Phys.* **29**, L205–206.

Cao, D. S., Stringfellow, G. B. (1990), *J. Electron. Mater.* **20**, 97–101.

Casey, H. C., Jr., Panish, M. B. (1978), *Heterostructure Lasers*, Orlando, FL: Academic.

Cook, L. W., Camras, M. D., Rudaz, S. L., Steranka, F. M. (1988), *Proceedings of the 14th International Symposium on GaAs and Related Compounds*, Bristol: Institute of Physics, pp. 777–780.

Craford, M. G. (1992), *Circuits Devices* **8**, 24–29.

Craford, M. G., Shaw, R. W., Groves, W. O., Herzog, A. H. (1972), *J. Appl. Phys.* **43**, 4075–4083.

Craford, M. G., Stillman, G. E., Holonyak, N., Jr., Rossi, J. A. (1991), *J. Electron. Mater.* **20**, 3–11.

Dawson, L. R. (1977), *J. Appl. Phys.* **48**, 2485–2492.

Dupuis, R. D., Dapkus, P. D. (1977), *Appl. Phys. Lett.* **31**, 466–468.

Edmond, J. A., Kong, H.-S., Carter, C. H., Jr. (1992), in: C. Y. Yang, M. M. Rahman, G. L. Harris (Eds.), *Amorphous and Crystalline Silicon Carbide IV*, Berlin: Springer, pp. 344–351.

Fletcher, R. M., Kuo, C. P., Osentowski, T. D., Huang, K. H., Craford, M. G. (1991), *J. Electron. Mater.* **20**, 1125–1130.

Fukuda, M. (1991), *Reliability and Degradation of Semiconductor Lasers and LEDs*, Boston: Artech House.

Groves, W. O., Herzog, A. H., Craford, M. G. (1971), *Appl. Phys. Lett.* **19**, 184–186.

Haase, M. A., Qiv, J., DePoydt, J. M., Cheng, H. (1991), *Appl. Phys. Lett.* **58**, 1272–1275.

Herzog, A. H., Groves, W. O., Craford, M. G. (1969), *Appl. Phys. Lett.* **40**, 1830–1838.

Herzog, A. H., Keune, D. L., Craford, M. G. (1972), *J. Appl. Phys.* **43**, 600–608.

Holonyak, N., Jr., Bevacqua, S. F. (1962), *Appl. Phys. Lett.* **1**, 82–83.

Huang, K. H., Yu, J. G., Kuo, C. P., Fletcher, R. M., Osentowski, T. D., Stinson, L. J., Liao, A. S. H., Craford, M.G. (1992), *Appl. Phys. Lett.* **61**, 1045–1047.

Jeon, J., Ding, J., Nurmikko, A.V., Xie, W., Kobayashi, M., Gunshor, R.L. (1992), *Appl. Phys. Lett.* **60**, 892–894.

Keyes, R. J., Quist, T. M. (1962), *Proc. IRE* **50**, 1822–1823.

Kimerling, L. C., Lang, D. V. (1975), in: F. A. Huntley (Ed.), *Lattice Defects in Semiconductors 1974*, Institute of Physics Conference Proceedings No. 23, Bristol, U.K.: Institute of Physics.

Kuo, C. P., Fletcher, R. M., Osentowski, T. D., Lardizabel, M. C., Craford, M. G. (1990), *Appl. Phys. Lett.* **57**, 2937–2939.

Logan, R. A., White, H. G., Wiegmann, W. (1968), *Appl. Phys. Lett.* **13**, 139–141.

Manasevit, H. M., Simpson, W. I. (1969), *J. Electrochem. Soc.* **116**, 1725–1732.

Nakamura, S., Mukai, T., Senoh, M. (1991a), *Jpn. J. Appl. Phys.* **30**, L1998–L2001.

Nakamura, S., Senoh, M., Mukai, T. (1991b), *Jpn. J. Appl. Phys.* **30**, L1701–L1711.

Nishizawa, J., Suto, K. (1977), *J. Appl. Phys.* **48**, 3484–3445.

Pearsall, T. P. (Ed.) (1982), *GaInAsP Alloy Semiconductors*, Chichester: Wiley.

Rupprecht, H., Woodall, J. M., Konnerth, K., Pettit, D. G. (1966), *Appl. Phys. Lett.* **9**, 221–223.

Rupprecht, H., Woodall, J. M., Pettit, G. D. (1967), *Appl. Phys. Lett.* **11**, 81–83.

Saul, R. H., Armstrong, J., Hackett, W. H., Jr. (1969), *Appl. Phys. Lett.* **15**, 229–231.

Saul, R.H., Lee, T. P., Burrus, C. A. (1985), in: W.T. Tsang (Ed.), *Semiconductors and Semimetals*, Orlando: Academic, Vol. 22, 193–237.

Sugawara, H., Ishikawa, M., Hatakoshi, G. (1991), *Appl. Phys. Lett.* **58**, 1010–1012.

Tannas, L. E., Jr. (1985), *Flat Panel Displays and CRTs*, New York: Van Nostrand Reinhold.

Xie, W., Grillo, D. C., Gunshor, R. L., Kobayashi, M., Jeon, H., Ding, J., Nurmikko, A. V., Hua, G. C., Otsuka, N. (1992), *Appl. Phys. Lett.* **60**, 1999–2001.

Further Reading

Bergh, A. A., Dean, P. J. (1976), *Light Emitting Diodes*, Oxford: Clarendon.

Casey, H. C., Jr., Panish, M. B. (1978), *Heterostructure Lasers*, Orlando, FL: Academic.

Craford, M. G. (1985), in: L. E. Tannas, Jr. (Ed.), *Flat-Panel Displays and CRTs*, New York: Van Nostrand Reinhold, pp. 289–331.

Gillessen, K., Schairer, W. (1987), *Light Emitting Diodes—An Introduction*, Englewood Cliffs, NJ: Prentice Hall.

Kressel, H., Butler, J. K. (1977), New York, *Semiconductor Lasers and Heterojunction LEDs*, Academic.

Saul, R. H., Lee, T. P., Burrus, C. A. (1985), in: W. T. Tsang (Ed.), *Semiconductors and Semimetals*, Orlando, FL: Academic, Vol. 22, pp. 193–237.

Williams, E. W., Hall, R. (1978), *Luminescence and the Light Emitting Diode*, Oxford: Pergamon.

LIGHT SCATTERING

See RAMAN SCATTERING

LINEAR ACCELERATORS

See ACCELERATORS, LINEAR

LINEAR ACOUSTICS

See ACOUSTICS, LINEAR

LINEAR OPTICS

See OPTICS, LINEAR

LIQUIDS

See ACOUSTIC PROPERTIES OF LIQUIDS; DIFFUSION AND IONIC CONDUCTION IN LIQUIDS; ELECTRON STRUCTURE OF LIQUIDS; MECHANICAL PROPERTIES OF LIQUIDS